

# ROOT SYSTEMS AND DIAGRAM CALCULUS.

## I. CYCLES IN THE CARTER DIAGRAMS

RAFAEL STEKOLSHCHIK

**ABSTRACT.** We consider admissible diagrams (a.k.a. Carter diagrams) introduced by R. Carter in 1972 for the classification of conjugacy classes in a finite Weyl group  $W$ . Cycles in the Carter diagrams are the focus of this paper. We show that the 4-cycles determine outcome. The explicit transformations of any Carter diagram containing long cycles ( $l > 4$ ) to another Carter diagram containing only 4-cycles are constructed. Thus all Carter diagrams containing long cycles can be discarded from the classification list. Conjugate elements of  $W$  give rise to the same diagram  $\Gamma$ . The converse is not true, as there exist diagrams determining two conjugacy classes in  $W$ . It is shown that the connected Carter diagram  $\Gamma$  containing at least one 4-cycle determines the single conjugacy class. We study a generalization of the Carter diagrams called connection diagrams.

### CONTENTS

<b>1. Introduction</b>	<b>3</b>
1.1. Admissible diagrams (a.k.a Carter diagrams)	4
1.2. Connection diagrams	5
1.2.1. Distinguishing acute and obtuse angles	5
1.2.2. Admissible and connection 4-cycles	5
1.3. The main results	6
1.4. Equivalence of connection diagrams	6
1.4.1. Three transformations of connection diagrams	6
1.4.2. Equivalence	7
1.4.3. Transformation of 4-cycles	7
1.5. Diagrams with 5 vertices and 5-cycles	8
<b>2. Classification of Carter diagrams</b>	<b>10</b>
2.1. For the multiply-laced case, only 4-cycle is possible	10
2.2. Two intersecting cycles in the simply-laced case	10
2.3. Classification of simply-laced Carter diagrams with cycles	12
2.3.1. The Carter diagrams with cycles on 6 vertices	12
2.3.2. The Carter diagrams with cycles on 7 vertices	14
2.3.3. The Carter diagrams with cycles on 8 vertices	14
2.3.4. The Carter diagrams with cycles on $l > 8$ vertices	16
<b>3. Exclusion of <math>n</math>-cycles, <math>n &gt; 4</math></b>	<b>16</b>
3.1. The pair of equivalent diagrams $\{E_8(b_3), E_8(a_3)\}$	16
3.2. The pair of equivalent diagrams $\{E_7(b_2), E_7(a_2)\}$ and $\{D_6(b_2), D_6(a_2)\}$	18
3.3. The pair of equivalent diagrams $\{E_8(b_5), E_8(a_5)\}$	19
3.4. The pair of equivalent diagrams $\{D_l(b_{\frac{l}{2}-1}), D_l(a_{\frac{l}{2}-1})\}$	21
3.4.1. The case $l = 4k$	22
3.4.2. The case $l = 4k - 2$	24
<b>4. The conjugacy class of the Carter diagram with a 4-cycle</b>	<b>26</b>
4.1. Uniqueness of the conjugacy class	26
4.2. Pair of orthogonal roots lying in 4-cycles	27
4.3. All 4-cycles are equivalent	27
4.4. The vertex with the branching degree $\geq 3$	28
4.5. The tail stemming from 4-cycle	29

4.6. Four patterns of root subsets	30
Appendix A. <b>Some properties of the Carter and Dynkin diagrams</b>	31
A.1. The ratio of lengths of roots	31
A.2. Cycles in simply-laced case	31
A.2.1. The Carter and connection diagrams for trees	31
A.2.2. There are no cycles for the diagram $A_n$	34
A.3. Cycles in the multiply-laced case	34
A.3.1. 4-cycle with all obtuse angles can not be	34
A.3.2. More impossible cases of multiply-laced cycles	35
A.4. Subsets of mutually orthogonal roots	36
References	38

The use of trees as diagrams for groups was anticipated in 1904, when C. Rodenberg [Rod04] was commenting on a set of models of cubic surfaces. He was analyzing the various rational double points that can occur on such a surface. In 1931, I used these diagrams in my enumeration of kaleidoscopes, where the dots represent mirrors. E.B.Dynkin re-invented the diagrams in 1946 for the classification of simple Lie algebras.

---

H. S. M. Coxeter, The evolution of Coxeter-Dynkin diagrams, [Cox91, p.224], 1991

## 1. Introduction

We consider *admissible diagrams* introduced by R. Carter in [Ca72, Section 4] for the classification of conjugacy classes in a finite Weyl group  $W$ . Any admissible diagram describes one or several conjugacy classes. Admissible diagrams generalize the Dynkin diagrams corresponding to the conjugacy class of the Coxeter element (Coxeter conjugacy class). Since the admissible diagrams characterize connections between not necessarily simple roots in the root systems associated with Dynkin diagrams, they may contain cycles. Cycles in the admissible diagrams are the focus of the paper. We show that among all cycles in admissible diagrams the 4-cycles (squares) determine the outcome. We also consider a certain generalization of admissible diagrams called *connection diagrams*. The precise definitions of admissible and connection diagrams will be given shortly, see Section 1.1 and Section 1.2. Intuitively, the differences between admissible and connection diagrams are as follows:

(a) any cycle in an admissible diagram contains an even number of vertices; this condition is not necessary for a connection diagram.

(b) the connection diagram is supplied together with an order  $\Omega$  of roots corresponding to vertices of the diagram; the order of roots for any admissible diagram is the fixed one associated with the bicolored decomposition of the element  $w$  characterized by this diagram, see (1.2).

Admissible and connection diagrams have several common properties: they both correspond to the set of linearly independent roots; these roots are not necessarily simple; any admissible and connection diagram describes an element  $w$  in the finite Weyl group  $W$  and the conjugacy class containing  $w$ . The following inclusions hold for the sets of Dynkin, admissible and connection diagrams:

$$\boxed{\text{Dynkin diagrams}} \subset \boxed{\text{Admissible diagrams}} \subset \boxed{\text{Connection diagrams}}$$

We consider a rather natural set of three transformations acting on a connection diagram and the root subset associated with this diagram, Section 1.4.1. Out of this set only conjugations preserve the diagrams. The other two transformations change connection diagrams; they preserve, however, the element  $w$  associated with the given diagram, see Table 1.1; all transformations preserve the conjugacy class containing  $w$ . The diagrams obtained (from one another) by these transformations are said to be *equivalent*. The admissible diagram may be equivalent to the connection diagram and vice versa. We widely use the method of equivalent diagrams:

(i) We exclude a number of admissible diagrams from Carter's list [Ca72, p. 10], namely all diagrams with cycles of length  $> 4$  can be excluded from the list since every such diagram is equivalent to a diagram containing only 4-cycles (Theorem 3.1).

(ii) We exclude a number of diagrams from the possible candidates of the admissible diagram since they have the subdiagram that is equivalent to extended Dynkin diagram, the case that can not be (Proposition A.2, Lemma 2.5).

(iii) Using several patterns of equivalent diagrams, we show that any Carter diagram containing a 4-cycle determines the single conjugacy class. Generally speaking, a Carter diagram determines one or more conjugacy classes in  $W$ , [Ca72, Lemma 27].

(iv) As a demonstration of the method of equivalent diagrams, we classify conjugacy classes associated with 5-cycles. According to the associated order, we get two Carter diagrams: one equivalent to the Carter diagram  $D_5(a_1)$ , and another equivalent to the Dynkin diagram  $D_5$  (Proposition 1.10).

(v) In [St11] we show that any connection diagram is equivalent to an admissible diagram. This statement implies the Carter theorem [Ca72, Theorem C]:

*Any element of a given finite Weyl group is expressible as the product of two involutions.*

**1.1. Admissible diagrams (a.k.a Carter diagrams).** Each element  $w \in W$  can be expressed in the form

$$w = s_{\alpha_1} s_{\alpha_2} \dots s_{\alpha_k}, \quad \alpha_i \in \Phi, \quad (1.1)$$

where  $\Phi$  is the root system associated with the Weyl group  $W$ ;  $s_{\alpha_i}$  are reflections in  $W$  corresponding to not necessarily simple roots  $\alpha_i \in \Phi$ . We denote by  $l_C(w)$  the smallest value  $k$  in any expression like (1.1). The Carter length  $l_C(w)$  is always less or equal to the classical length  $l(w)$ . The decomposition (1.1) is called *reduced* if  $l_C(s_{\alpha_1} s_{\alpha_2} \dots s_{\alpha_k}) = k$ .

**Lemma 1.1.** [Ca72, Lemma 3] *Let  $\alpha_1, \alpha_2, \dots, \alpha_k \in \Phi$ . Then  $s_{\alpha_1} s_{\alpha_2} \dots s_{\alpha_k}$  is reduced if and only if  $\alpha_1, \alpha_2, \dots, \alpha_k$  are linearly independent.*

**Lemma 1.2.** [Ca72, Lemma 5] *Every involution  $w \in W$  can be expressed as a product of  $l_C(w)$  reflections corresponding to mutually orthogonal roots*

Suppose  $w = w_1 w_2$  is the decomposition of  $w$  into the product of two involutions. By Lemma 1.2, we have:

$$w_1 = s_{\alpha_1} s_{\alpha_2} \dots s_{\alpha_k}, \quad w_2 = s_{\beta_1} s_{\beta_2} \dots s_{\beta_h}, \quad k + h = l_C(w). \quad (1.2)$$

where  $\{\alpha_1, \alpha_2, \dots, \alpha_k\}$ , (resp.  $\{\beta_1, \beta_2, \dots, \beta_h\}$ ) forms the set of mutually orthogonal roots. Again,  $\alpha_i$  and  $\beta_j$  in (1.2) are not necessarily simple roots in  $\Phi$ . We denote by  $\alpha$ -set (resp.  $\beta$ -set) the subset of roots corresponding to  $w_1$  (resp.  $w_2$ ):

$$\alpha\text{-set} = \{\alpha_1, \alpha_2, \dots, \alpha_k\}, \quad \beta\text{-set} = \{\beta_1, \beta_2, \dots, \beta_h\}. \quad (1.3)$$

We call the decomposition (1.2) the *bicolored* decomposition.

An admissible diagram  $\Gamma$  is any diagram satisfying two conditions:

- (a) The nodes of  $\Gamma$  correspond to a set of linearly independent roots in the Weyl group  $W$ .
- (b) Each subdiagram of  $\Gamma$  which is a cycle contains an even number of vertices.

Every reduced bicolored decomposition is associated with the admissible diagram. By Lemma 1.1 the condition (a) holds. For the bicolored decomposition, the condition (b) holds. Indeed, let us fix, for example, the clockwise orientation of the cycle. Then any  $\alpha_i$  from the  $\alpha$ -set is connected in the clockwise direction exactly to one element  $\beta_i$  from the  $\beta$ -set, and the number of vertices of the cycle is even.

Admissible diagrams are also called *Carter diagrams*, see [DF95], [Wi05], [DI09]. From now on, we call them the Carter diagrams.

**Remark 1.3** (Primitive (semi-Coxeter) conjugacy class). A conjugacy class of  $W$  that can be described by a connected Carter diagram with number of nodes equal to the rank of  $W$  is called a *semi-Coxeter conjugacy class*, [CE72], or, more frequently, a *primitive conjugacy class*, [KP85], [DF95], [Sev09], [B89]. The conjugacy class, whose Carter diagram is the Dynkin diagram of  $W$ , is called the *Coxeter conjugacy class*. Any representative of the primitive (semi-Coxeter) conjugacy class is called a *primitive element*, or a *semi-Coxeter element* [KP85], [B89], [St11].

**1.2. Connection diagrams.** The connection diagram is the pair  $(\Gamma, \Omega)$ , where  $\Gamma$  is the diagram characterizing connections between roots as they are characterized by Dynkin diagram or by the Carter diagram, and  $\Omega$  is an order of elements in the decomposition (1.1) that is not necessarily bicolored. As in the case of Carter diagrams, roots associated with a connection diagram are linearly independent and are not necessarily simple. We omit order  $\Omega$  in the description of the connection diagram if the order is clear from the decomposition like (1.1). The connection diagram describes the element  $w$  (and its inverse  $w^{-1}$ ) obtained as the product of all reflections associated with the diagram, the order  $\Omega$  (resp.  $\Omega^{-1}$ ) describes the order of reflections in  $w$  (resp.  $w^{-1}$ ). Similarly to Remark 1.3, we call  $w$  the *primitive element associated with the connection diagram*  $(\Gamma, \Omega)$ , or  $(\Gamma, \Omega)$ -*primitive element*.

**1.2.1. Distinguishing acute and obtuse angles.** Recall that for the Dynkin diagrams, all angles between simple roots are obtuse and there is no need for a special denotation. For the Carter diagrams and connection diagrams, we add the special denotation to distinguish acute and obtuse angles between roots. A *solid edge* indicates an obtuse angle between the roots exactly as for Dynkin diagrams. A *dotted edge* indicates an acute angle between the roots considered, see Fig. 1.1.

**1.2.2. Admissible and connection 4-cycles.** The Carter diagram for 4-cycle in Fig. 1.1 describes the bicolored decomposition:

$$w = s_{\alpha_1} s_{\alpha_2} s_{\beta_1} s_{\beta_2}.$$

Here,  $w$  is the primitive element associated with the Carter diagram  $D_4(a_1)$ , i.e.,  $w$  is the  $D_4(a_1)$ -primitive element. In the case of Carter diagrams the order is trivial and we omit it. The connection diagram in Fig. 1.1 is supplied with the order  $\Omega = \{\alpha_1, \beta_1, \alpha_2, \beta_2\}$ :

$$w_\Omega = s_{\alpha_1} s_{\beta_1} s_{\alpha_2} s_{\beta_2}. \quad (1.4)$$

In (1.4),  $w_\Omega$  is the primitive element associated with the diagram  $(\mathcal{G}_4, \Omega)$ , where  $\mathcal{G}_4$  is a 4-cycle. We will omit the index of the element  $w_\Omega$  if the order  $\Omega$  is clear from the context.

**Remark 1.4.** Hereafter, we suppose that every cycle contains only one dotted edge. Otherwise, we apply reflections  $\alpha \rightarrow -\alpha$ . These operations do not change the element  $w$  since  $s_\alpha = s_{-\alpha}$ . In this case, every dotted edge with the vertex  $\alpha$  is changed to the solid one. The cycle with all edges solid can not occur, see Lemma A.1. Also note that the dotted edge can be moved to any other edge of the cycle by means of reflections.

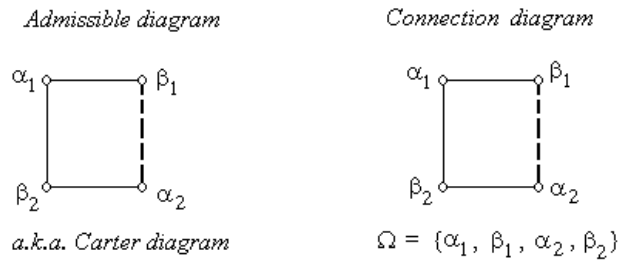


Figure 1.1. Admissible diagram (a.k.a. Carter diagram) and connection diagram for 4-cycle

The primitive elements generated by reflections  $s_{\alpha_1}, s_{\alpha_2}, s_{\beta_1}, s_{\beta_2}$  constitute exactly two conjugacy classes;  $w$  and  $w_\Omega$  are representatives of these classes. In the basis  $\{\alpha_1, \alpha_2, \beta_1, \beta_2\}$ , we have:

$$w = \begin{pmatrix} 1 & 0 & -1 & -1 \\ 0 & 1 & 1 & -1 \\ 1 & -1 & -1 & 0 \\ 1 & 1 & 0 & -1 \end{pmatrix}, \quad w_\Omega = \begin{pmatrix} 0 & 1 & 0 & 0 \\ 1 & 0 & -1 & -1 \\ 0 & 0 & 0 & 1 \\ 1 & 1 & 0 & -1 \end{pmatrix} \quad (1.5)$$

and their characteristic polynomials are:

$$\chi(w) = x^4 + 2x^2 + 1, \quad \chi(w_\Omega) = x^4 + x^3 + x + 1. \quad (1.6)$$

**1.3. The main results.** In Section 2, we go behind Carter's classification of his diagrams. We add new arguments to get Carter's classification, namely we use the method of equivalent diagrams and the following:

**Proposition** (on intersecting cycles (Proposition 2.3)) *Two intersecting cycles belonging to a Carter diagram or to a connection diagram have the intersection which consists of exactly one edge.*

The main part, the classification of the simply-laced Carter diagrams with cycles, is given in Section 2.3, see Table 2.3. In Section 3, we exclude all diagrams with cycles of length  $> 4$ . (This fact is taken into account in the classification of Section 2.3).

**Theorem** (on the exclusion of long cycles (Theorem 3.1)) *Any Carter diagram containing  $l$ -cycles ( $l > 4$ ) is equivalent to another Carter diagram containing only 4-cycles.*

For the proof, we construct the explicit transformation of the element  $w$  described by the Carter diagram  $\Gamma$  containing  $l$ -cycles ( $l > 4$ ) to an element  $w'$  from the same conjugacy class described by another Carter diagram  $\Gamma'$  containing only 4-cycles. The meaning of Theorem 3.1 is that all Carter diagrams, containing long cycles ( $l > 4$ ) may be discarded from the classification list, [Ca72, Table 1].

**Remark 1.5.** A hint to validity of Theorem 3.1 can be found in the coincidence of the characteristic polynomials of primitive elements corresponding to every element of the pair in Table 3.4, [Ca72, Table 3], see also [CE72, p. 252].  $\square$

In Section 4, we show that all 4-cycles in the same Weyl group are equivalent. (Proposition 4.5). Several other patterns of equivalent diagrams are considered. Conjugate elements of  $W$  are associated with the same diagram  $\Gamma$ . The converse is not true, the diagram  $\Gamma$  does not determine a single conjugacy class in  $W$ , [Ca72, Lemma 27]. The following theorem gives the sufficient condition of the uniqueness of the conjugacy class determined by the diagram  $\Gamma$ :

**Theorem** (on the conjugacy class of the diagram (Theorem 4.1)) *Let  $\Gamma$  be a connected Carter diagram containing at least one 4-cycle. Then  $\Gamma$  determines only one conjugacy class.*

#### 1.4. Equivalence of connection diagrams.

**1.4.1. Three transformations of connection diagrams.** For every decomposition  $w = s_{\alpha_1} s_{\alpha_2} \dots s_{\alpha_n}$ , where  $s_{\alpha_i}$  for  $i = 1, 2, \dots, n$  are reflections in the Weyl group  $W$ , we assign the order  $\Omega$  of roots  $\Omega = \alpha_1, \alpha_2, \dots, \alpha_n$ , and  $w = w_\Omega$ :

$$w = s_{\alpha_1} s_{\alpha_2} \dots s_{\alpha_n} \iff \Omega = \{\alpha_1, \alpha_2, \dots, \alpha_n\}. \quad (1.7)$$

Two orders  $\Omega_1$  and  $\Omega_2$  derivable from one another by the permutation of adjacent roots  $\alpha_i, \alpha_{i+1}$  are equivalent  $\Omega_1 \simeq \Omega_2$  if the corresponding reflections commute:  $s_{\alpha_i} s_{\alpha_{i+1}} = s_{\alpha_{i+1}} s_{\alpha_i}$ . The transformation of the element  $w = w_\Omega$  from (1.7) is equivalent to the transformation of the connection diagram  $(\Gamma, \Omega)$ .

We consider three types of transformations applicable to connection diagrams:

(I) conjugation:  $w \longrightarrow wuw^{-1}$ , where  $u \in W$ . The order  $\Omega$  is changed as follows:

$$w \longrightarrow wuw^{-1} = s_{u\alpha_1} s_{u\alpha_2} \dots s_{u\alpha_n} \iff \{u\alpha_1, u\alpha_2, \dots, u\alpha_n\}. \quad (1.8)$$

(II)  $s$ -permutation:  $s_\alpha s_\beta = s_{s_\alpha(\beta)} s_\alpha = s_\beta s_{s_\beta(\alpha)}$ . In this case, we have

$$\begin{aligned} w = s_{\alpha_1} \dots s_{\alpha_i} s_{\alpha_{i+1}} \dots s_{\alpha_n} &\iff \{\alpha_1, \dots, \alpha_i, \alpha_{i+1}, \dots, \alpha_n\}, \\ w = s_{\alpha_1} \dots s_{s_{\alpha_i}(\alpha_{i+1})} s_{\alpha_i} \dots s_{\alpha_n} &\iff \{\alpha_1, \dots, s_{\alpha_i}(\alpha_{i+1}), \alpha_i, \dots, \alpha_n\}, \\ w = s_{\alpha_1} \dots s_{\alpha_{i+1}} s_{s_{\alpha_{i+1}}(\alpha_i)} \dots s_{\alpha_n} &\iff \{\alpha_1, \dots, \alpha_{i+1}, s_{\alpha_{i+1}}(\alpha_i), \dots, \alpha_n\}. \end{aligned} \quad (1.9)$$

(III)  $s_\alpha$ -reflection:  $\alpha \longrightarrow -\alpha$ ;  $s_\alpha = s_{-\alpha}$ . In this case, every dotted edge with vertex  $\alpha$  is changed to the solid one and vice versa.

Operation	Preserves	Changes
conjugation $w \longrightarrow u w u^{-1}$	connection diagram	$w$
$s$ -permutation $s_\alpha s_\beta = s_{s_\alpha(\beta)} s_\alpha = s_\beta s_{s_\beta(\alpha)}$	$w$	connection diagram
$s_\alpha$ -reflection $\alpha \longrightarrow -\alpha; s_\alpha = s_{-\alpha}$	$w$	connection diagram

Table 1.1. Operations preserving conjugacy classes and changing the connection diagram to an equivalent one (see Section 1.4.1).

**Remark 1.6** (on trees). For the set  $\{\alpha_1, \dots, \alpha_i, \alpha_{i+1}, \dots, \alpha_n\}$  forming a tree, we may assume that all non-zero inner products  $(\alpha_i, \alpha_j)$  are negative. Indeed, if  $(\alpha_i, \alpha_j) > 0$ , we change  $\alpha_j \longrightarrow -\alpha_j$ , and now we consider all inner products  $(\alpha_k, \alpha_j) > 0$  and repeat the change  $\alpha_k \longrightarrow -\alpha_k$  if necessary. This process converges since the diagram is the tree.

**Lemma 1.7.** *Let  $A = \{\alpha_1, \alpha_2, \dots, \alpha_n\} \subset \Phi$  be the set of linearly independent vectors. Transformations (I), (II), (III) preserve the linear independency of  $A$ .*

It is easily derived from (1.8) and (1.9).  $\square$

1.4.2. *Equivalence.* Transformations (I), (II), (III) are said to be *equivalent transformations* of the diagram  $(\Gamma, \Omega)$ . We say that connection diagrams  $(\Gamma_1, \Omega_1)$  and  $(\Gamma_2, \Omega_2)$  are *equivalent* if each of them can be obtained from the other one by a certain sequence of transformations (I), (II), (III) from Section 1.4.1. In this case we write:

$$(\Gamma_1, \Omega_1) \simeq (\Gamma_2, \Omega_2). \quad (1.10)$$

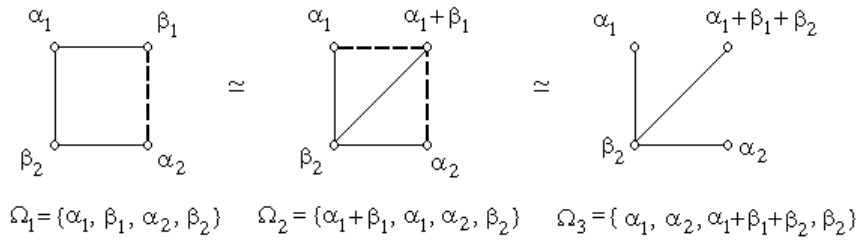


Figure 1.2. Elimination of the cycle. Equivalence of  $(\mathcal{G}_4, \Omega_1)$  and  $(D_4, \Omega_3)$

1.4.3. *Transformation of 4-cycles.* Let us transform the element  $w_\Omega$  from (1.4):

$$w_\Omega = s_{\alpha_1} s_{\beta_1} s_{\alpha_2} s_{\beta_2} = s_{\alpha_1 + \beta_1} s_{\alpha_1} s_{\alpha_2} s_{\beta_2} \stackrel{s_{\alpha_1 + \beta_1}}{\simeq} s_{\alpha_1} s_{\alpha_2} s_{\beta_2} s_{\alpha_1 + \beta_1} = s_{\alpha_1} s_{\alpha_2} s_{\alpha_1 + \beta_1 + \beta_2} s_{\beta_2} \quad (1.11)$$

(we denote by  $\stackrel{u}{\simeq}$  the conjugation  $w \longrightarrow u w u^{-1}$ ). We have:

$$\begin{aligned}
 (\alpha_1 + \beta_1 + \beta_2, \alpha_1) &= (\alpha_1, \alpha_1) + (\beta_1, \alpha_1) + (\beta_2, \alpha_1) = 1 - \frac{1}{2} - \frac{1}{2} = 0, \text{ and} \\
 (\alpha_1 + \beta_1 + \beta_2, \alpha_2) &= (\beta_1, \alpha_2) + (\beta_2, \alpha_2) = -\frac{1}{2} + \frac{1}{2} = 0.
 \end{aligned} \quad (1.12)$$

Thus,  $\{\alpha_1, \alpha_2, \alpha_1 + \beta_1 + \beta_2\}$  constitute the triple of orthogonal roots, and we obtained in (1.11) the bicolored decomposition. Thus, we reduced the connection diagram  $(\mathcal{G}_4, \Omega_1)$  to the Carter diagram  $(D_4, \Omega_3)$ , see Fig. 1.2. That is why, in (1.6) the characteristic polynomial  $\chi(w_{\Omega_1}) = x^4 + x^3 + x + 1 = (x^3 + 1)(x + 1)$  is equal to the characteristic polynomial of the primitive element for  $D_4$ , see [Ca72, Table 3], or [St08, Table 1].

**1.5. Diagrams with 5 vertices and 5-cycles.** There are root subsets forming 5-cycles, though 5-cycles are not the Carter diagrams. For example, the root subset

$$\{e_1 - e_2, e_2 - e_3, e_3 - e_4, e_4 - e_5, e_1 + e_5\}$$

from the root systems  $D_n, E_n, n \geq 5$  constitutes the cycle of length 5. However, any 5-cycle can be equivalently transformed to the diagram containing only 4-cycle or diagram without cycles.

**Lemma 1.8.** *Let  $(\Gamma, \Omega)$  be the 5-vertex diagram consisting of the 4-cycle and 3-cycle (as in Fig. 1.3). Up to equivalence, there are only 2 different elements  $w_\Omega$  (and the associated connection diagrams  $(\Gamma, \Omega)$ ), see Fig. 1.3 and Fig. 1.4.*

*Proof.* Note that two diagrams  $(\Gamma, \Omega_1)$  and  $(\Gamma, \Omega_2)$  are equivalent if orders  $\Omega_1$  and  $\Omega_2$  differ only by the cyclic permutation of vertices. Then onto the first place we put the element  $\gamma$  lying in the 3-cycle, and not the one lying in the 4-cycle, see Fig. 1.3. There are two cases:

1) The diagonal elements  $(\alpha_1, \alpha_2)$  of the 4-cycle are adjacent, or can be transformed to an adjacent pair by equivalent transformations of  $(\Gamma, \Omega)$ . Then the same applies to the other pair of diagonal elements  $(\beta_1, \beta_2)$ .

2) The diagonal elements  $(\alpha_1, \alpha_2)$  (resp.  $(\beta_1, \beta_2)$ ) are not adjacent and cannot be transformed to an adjacent pair by any equivalent transformation.

*Case 1).* For the diagram  $(\Gamma, \Omega)$ , where  $\Omega = \{\gamma, \alpha_1, \alpha_2, \beta_1, \beta_2\}$ , the element  $w_\Omega$  is as follows:

$$w_\Omega = s_\gamma s_{\alpha_1} s_{\alpha_2} s_{\beta_1} s_{\beta_2} = s_\gamma s_{\alpha_1} s_{\beta_1} s_{\beta_2} s_{\alpha_2 - \beta_1 + \beta_2},$$

where

$$(\alpha_2 - \beta_1 + \beta_2, \alpha_1) = 0,$$

$$(\alpha_2 - \beta_1 + \beta_2, \gamma) = 0,$$

$$(\alpha_2 - \beta_1 + \beta_2, \beta_1) = -1 + \frac{1}{2} = -\frac{1}{2},$$

$$(\alpha_2 - \beta_1 + \beta_2, \beta_2) = 1 - \frac{1}{2} = \frac{1}{2}.$$

Hence,

$$w_\Omega \stackrel{s_{\alpha_1}}{\simeq} s_\gamma s_{\beta_1} s_{\beta_2} s_{\alpha_2 - \beta_1 + \beta_2} s_{\alpha_1}.$$

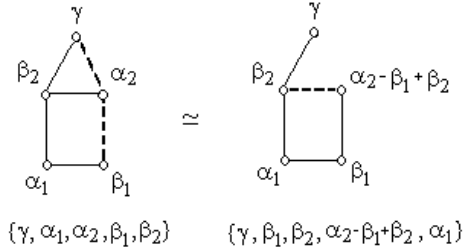


Figure 1.3.

*Case 2).* For the diagram  $(\Gamma, \Omega)$ , where  $\Omega = \{\gamma, \alpha_1, \beta_1, \alpha_2, \beta_2\}$ , the element  $w_\Omega$  is as follows:

$$w_\Omega = s_\gamma s_{\alpha_1} s_{\beta_1} s_{\alpha_2} s_{\beta_2} =$$

$$s_\gamma s_{\alpha_1} s_{\beta_1} s_{\beta_2} s_{\beta_2 + \alpha_2} \stackrel{s_{\alpha_1}}{\simeq}$$

$$s_\gamma s_{\beta_1} s_{\beta_2} s_{\beta_2 + \alpha_2} s_{\alpha_1} =$$

$$s_\gamma s_{\beta_1} s_{\beta_2} s_{\alpha_1} s_{\beta_2 + \alpha_2 + \alpha_1},$$

where

$$(\beta_2 + \alpha_2 + \alpha_1, \alpha_1) = 1 - \frac{1}{2} = \frac{1}{2},$$

$$(\beta_2 + \alpha_2 + \alpha_1, \gamma) = 0,$$

$$(\beta_2 + \alpha_2 + \alpha_1, \beta_1) = 0,$$

$$(\beta_2 + \alpha_2 + \alpha_1, \beta_2) = 0.$$

The lemma is proved.  $\square$

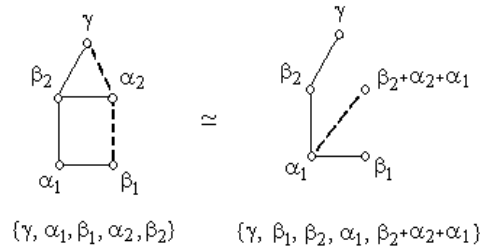


Figure 1.4.



**Remark 1.9.** Let  $\mathbf{C}_\Lambda$  be the Coxeter element associated with an orientation  $\Lambda$ , [St08, Section 2.2.6]. For the case, where diagram  $\Gamma$  is a cycle, Menshikh and Subbotin established a connection between an orientation  $\Lambda$  of  $\Gamma$  and the conjugacy class of the Coxeter element, [Men85]. They considered an invariant  $R_\Lambda$  equal to the number of arrows directed clockwise, and showed that two Coxeter transformations  $\mathbf{C}_{\Lambda_1}$  and  $\mathbf{C}_{\Lambda_2}$  are conjugate if  $R_{\Lambda_1} = R_{\Lambda_2}$ . Note that  $R_{\Lambda_1} = R_{\Lambda_2}$  if and only if orientations  $\Lambda_1$  and  $\Lambda_2$  can be obtained from each other by applying a sink-admissible (or source-admissible) sequence of reflections, see [BGP73], [St08, p.73]. The two orientations, all whose arrows directed clockwise (resp. counterclockwise) are excluded. For 5-cycles, there are 4 types of orientations associated with  $R_\Lambda = 1, 2, 3, 4$ . In the following proposition we show that there are only 2 conjugacy classes of Coxeter elements characterized by Carter diagrams  $D_5$  and  $D_5(a_1)$ .

**Proposition 1.10.** *There are 2 conjugacy classes of Coxeter elements for 5-cycles, namely:*

- 1) *For  $R_\Lambda = 1$  or 4, the Coxeter element associated with a given orientation of 5-cycle conjugate to the primitive element associated with the Dynkin diagram  $D_5$ , see Table 1.2.*
- 2) *For  $R_\Lambda = 2$  or 3, the Coxeter element associated with a given orientation of 5-cycle conjugate to the primitive element associated with the Carter diagram  $D_5(a_1)$ , see Table 1.2.*

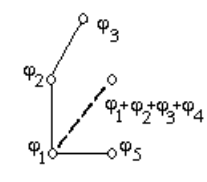
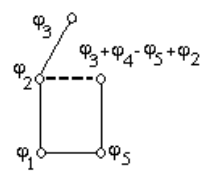
Element $w_\Omega$ (up to conjugation)	Index $R_\Lambda$	The primitive element $w_0$ conjugate to $w_\Omega$	The equivalent Carter diagram
$s_{\varphi_1} s_{\varphi_5} s_{\varphi_4} s_{\varphi_3} s_{\varphi_2}$ $s_{\varphi_1} s_{\varphi_2} s_{\varphi_3} s_{\varphi_4} s_{\varphi_5}$	$R_\Lambda = 1$ $R_\Lambda = 4$	$(s_{\varphi_2+\varphi_3+\varphi_4+\varphi_1} s_{\varphi_5} s_{\varphi_2})(s_{\varphi_3} s_{\varphi_1})$	 $D_5$
$s_{\varphi_1} s_{\varphi_2} s_{\varphi_5} s_{\varphi_4} s_{\varphi_3}$ $s_{\varphi_1} s_{\varphi_3} s_{\varphi_4} s_{\varphi_5} s_{\varphi_2}$	$R_\Lambda = 2$ $R_\Lambda = 3$	$(s_{\varphi_5} s_{\varphi_2})(s_{\varphi_3+\varphi_4-\varphi_5+\varphi_2} s_{\varphi_1} s_{\varphi_3})$	 $D_5(a_1)$

Table 1.2. The bicolored decompositions  $w_0$  for 2 conjugacy classes of Coxeter elements associated with 5-cycles

*Proof.* Case  $R_\Lambda = 1$ . The order  $\Omega = \{\varphi_1, \varphi_5, \varphi_4, \varphi_3, \varphi_2\}$ , and  $w_\Omega$  is as follows:

$$\begin{aligned}
 s_{\varphi_1} s_{\varphi_5} s_{\varphi_4} s_{\varphi_3} s_{\varphi_2} &= s_{\varphi_1} s_{\varphi_5} s_{\varphi_3} s_{\varphi_3+\varphi_4} s_{\varphi_2} \stackrel{s_{\varphi_1}}{\simeq} \\
 s_{\varphi_3} s_{\varphi_5} s_{\varphi_3+\varphi_4} s_{\varphi_2} s_{\varphi_1} &= \\
 s_{\varphi_3} s_{\varphi_5} s_{\varphi_2} s_{\varphi_1} s_{\varphi_3+\varphi_4+\varphi_2+\varphi_1} &\stackrel{s_{\varphi_3}}{\simeq} \\
 (s_{\varphi_5} s_{\varphi_2})(s_{\varphi_1} s_{\varphi_3}) s_{\varphi_3+\varphi_4+\varphi_2+\varphi_1} &\stackrel{s_{\varphi_3+\varphi_4+\varphi_2+\varphi_1}}{\simeq} \\
 (s_{\varphi_3+\varphi_4+\varphi_2+\varphi_1} s_{\varphi_5} s_{\varphi_2})(s_{\varphi_1} s_{\varphi_3}). &
 \end{aligned}$$

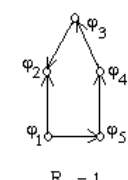
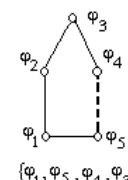
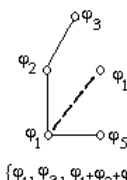

 $R_\Lambda = 1$ 

 $\{\varphi_1, \varphi_5, \varphi_4, \varphi_3, \varphi_2\}$ 
 $\simeq$ 

 $\{\varphi_1, \varphi_3, \varphi_1+\varphi_2+\varphi_3+\varphi_4, \varphi_5, \varphi_2\}$

Figure 1.5.

Note that vectors  $\varphi_2$ ,  $\varphi_5$  and  $\varphi_3 + \varphi_4 + \varphi_2 + \varphi_1$  are mutually orthogonal. Similarly, we get the same decomposition for the case  $R_\Lambda = 4$  corresponding to the inverse order  $\Omega^{-1} = \{\varphi_2, \varphi_3, \varphi_4, \varphi_5, \varphi_1\}$ .

Case  $R_\Lambda = 2$ . The order  $\Omega = \{\varphi_1, \varphi_2, \varphi_5, \varphi_4, \varphi_3\}$ . We have the following element  $w_\Omega$ :

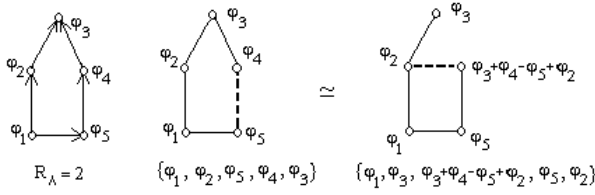


Figure 1.6.

Vectors  $\varphi_1$ ,  $\varphi_3$  and  $\varphi_3 + \varphi_4 - \varphi_5 + \varphi_2$  are mutually orthogonal. Similarly, we get the same decomposition for the case  $R_A = 3$  corresponding to the inverse order  $\Omega^{-1} = \{\varphi_3, \varphi_4, \varphi_5, \varphi_2, \varphi_1\}$ .  $\square$

**Acknowledgements.** I am grateful to Leonid Kontorovich and Len Zheleznyak for the English editing that helped me to improve this paper.

## 2. Classification of Carter diagrams

In this section, we add new arguments to obtain Carter's list of his diagrams: we use the statement on intersecting cycles, Proposition 2.3; we exclude diagrams with cycles of length  $> 4$ , see Theorem 3.1.

The following proposition states that any Carter diagram or connection diagram without cycles is a Dynkin diagram.

**Proposition 2.1** (Lemma 8, [Ca72]). *Let  $S = \{\alpha_1, \dots, \alpha_n\} \subset \Phi$  be the set of linearly independent (not necessarily simple) roots, and let  $\Gamma$  be the Carter diagram or the connection diagram associated with the set  $S$ . If  $\Gamma$  is a tree, then  $\Gamma$  is the Dynkin diagram.*

For the proof and examples, see Section A.2.1.  $\square$

Due to this proposition, for the proof of the Carter theorem (see Section 1,(v)), it suffices to consider only diagrams with cycles.

**Remark 2.2.** For  $G_2$  and  $A_n$ , there are no Carter diagrams with cycles.

- 1) For  $G_2$ , this fact is trivial, since there are maximum two linearly independent roots.
- 2) For case  $A_n$ , see A.2.2.

**2.1. For the multiply-laced case, only 4-cycle is possible.** Consider a multiply-laced diagram containing cycles. If the root system  $\Phi$  contains a cycle, then  $\Phi$  constitutes the 4-cycle with one dotted edge, [Ca72, p. 13]. This case occurs in  $F_4$ , see Fig. 2.7. In Section A.3, we prove that for multiply-laced cases, there are no other Carter diagrams with cycles.

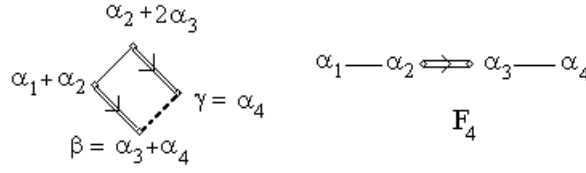
If  $\alpha_1, \alpha_2, \alpha_3, \alpha_4$  are the simple roots in  $F_4$ , then the quadruple

$$\alpha = \alpha_1 + \alpha_2, \quad \beta = \alpha_3 + \alpha_4, \quad \gamma = \alpha_4, \quad \delta = \alpha_2 + 2\alpha_3$$

constitutes such a 4-cycle. Values of the Tits form on the corresponding pairs of roots are as follows:

$$\begin{aligned} (\alpha, \beta) &= (\alpha_1 + \alpha_2, \alpha_3 + \alpha_4) = (\alpha_2, \alpha_3) = -1, \\ (\beta, \gamma) &= (\alpha_3 + \alpha_4, \alpha_4) = (\alpha_4, \alpha_4) - (\alpha_3, \alpha_4) = 1 - \frac{1}{2} = \frac{1}{2} \quad (\text{dotted edge}), \\ (\gamma, \delta) &= (\alpha_4, \alpha_2 + 2\alpha_3) = 2(\alpha_4, \alpha_3) = -1, \\ (\delta, \alpha) &= (\alpha_2 + 2\alpha_3, \alpha_1 + \alpha_2) = (\alpha_2, \alpha_2) + (\alpha_2, \alpha_1) + 2(\alpha_2, \alpha_3) = 2 - 1 - 2 = -1. \end{aligned}$$

**2.2. Two intersecting cycles in the simply-laced case.** From the foregoing, in Section 2, it is sufficient to consider only simply-laced diagrams. First of all, we discuss Carter diagrams containing exactly two intersecting cycles. The expression “intersection of two cycles” means the common path of these cycles. If there are two candidates for a common path of the same length, the choice does not matter.


 Figure 2.7. 4-cycle root subset in  $F_4$ . The angle  $(\widehat{\beta, \gamma})$  is acute

**Proposition 2.3** (intersection of two cycles). 1) Let  $\Gamma$  be any Carter diagram or connection diagram containing two cycles intersecting among the path  $\mathcal{F}$ . Then the path  $\mathcal{F}$  consists of exactly one edge.

2) Let  $\Gamma$  be any Carter diagram. Let  $C_1, C_2 \subset \Gamma$  be two paths stemming from the opposite vertices of a 4-cycle in  $\Gamma$ ; let  $\alpha_1$  (resp.  $\alpha_2$ ) be the vertex lying in  $C_1$  (resp.  $C_2$ ). The diagram obtained from  $\Gamma$  by adding the edge  $\{\alpha_1, \alpha_2\}$  is not a Carter diagram, see Fig. 2.9.

3) Let  $\Gamma$  be any Carter diagram containing two intersecting cycles. Then one of the cycles consists of 4 vertices, and the other one can contain only 4 or 6 edges.

*Proof.* 1) Every cycle contains odd dotted edges, otherwise it may be achieved by reflections in some vertices, Lemma A.1. Let  $n_1$  be the odd number of dotted edges in the top cycle:  $\{\alpha_1, \beta_1, \alpha_2, \beta_2, \alpha_3, \beta_n\}$ ,  $n_2$  be the odd number of dotted edges in the bottom cycle:  $\{\alpha_4, \beta_1, \alpha_2, \beta_2, \alpha_5, \beta_m\}$ . Suppose the intersection of the top and bottom cycles contains a common vertex  $\alpha_2$  (in Fig. 2.8 this intersection is the chain  $\{\beta_1, \alpha_2, \beta_2\}$ ). After discarding the vertex  $\alpha_2$  we get a bigger cycle; let  $n_3$  be the odd number of dotted edges in the bigger cycle  $\{\alpha_1, \beta_1, \alpha_4, \beta_m, \alpha_5, \beta_2, \alpha_3, \beta_n\}$ . Therefore  $n_1 + n_2 + n_3$  is odd. On the other hand, every dotted edge enters twice, so  $n_1 + n_2 + n_3$  is even. Thus, there is no vertex in the intersection  $\{\beta_1, \beta_2\}$  of the two cycles.

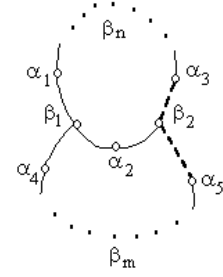


Figure 2.8.

2) The diagram  $\Gamma \cup \{\alpha_1, \alpha_2\}$  contains the intersection  $\{\beta_1, \gamma, \beta_2\}$  of length 2, see figure:

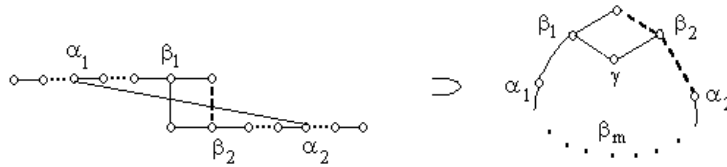


Figure 2.9. Two paths stemming from the opposite vertices of a 4-cycle

Thus by 1) the diagram  $\Gamma \cup \{\alpha_1, \alpha_2\}$  is not a Carter diagram.

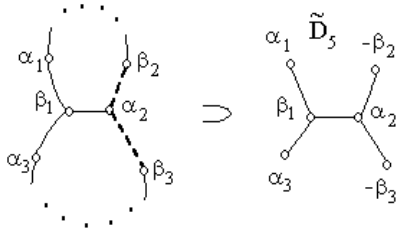


Figure 2.10.

3) By 1) the intersection of the two cycles consists of one edge  $\{\beta_1, \alpha_2\}$ , see Fig. 2.10. Then at least one of the cycles is of length 4. Otherwise, the Carter diagram contains the extended Dynkin diagram  $\tilde{D}_5$  contradicting Proposition A.2. As above, the dotted edge may be eliminated in  $\tilde{D}_5$  by changing the sign of one of the roots.

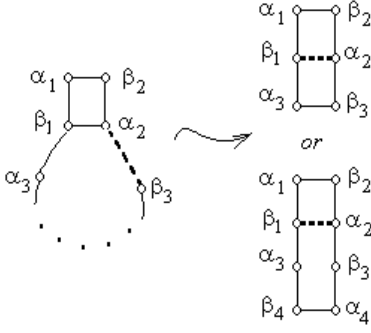


Figure 2.11.

The second cycle can be only of length 4 or 6 as in Fig. 2.11. It cannot be a cycle of length 8, otherwise the Carter diagram contains the extended Dynkin diagram  $\tilde{E}_7$ , see Fig. 2.12. According to heading 2), we can not add edges  $\{\alpha_1, \beta_3\}$ ,  $\{\alpha_1, \beta_5\}$ ,  $\{\beta_2, \alpha_3\}$ , or  $\{\beta_2, \alpha_5\}$ .

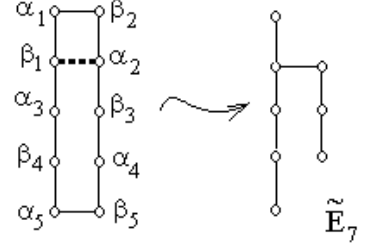


Figure 2.12.

□

**Corollary 2.4.** 1) Let an  $\alpha$ -set contain 3 roots  $\{\alpha_1, \alpha_2, \alpha_3\}$ . There does not exist two non-connected roots  $\beta$  and  $\gamma$  connected to every  $\alpha_i$ .

2) Let  $\{\alpha_1, \beta_1, \alpha_2, \beta_2\}$  be a square in a connection diagram. There does not exist a root  $\gamma$  connected to all vertices of the square.

*Proof.* 1) Let there be three  $\alpha$ -endpoints (see, for example, Fig. 2.13). Then we have three

cycles:  $\{\alpha_i, \gamma, \alpha_j, \beta\}$ , where  $1 \leq i < j \leq 3$ . Every cycle should contain an odd number of dotted edges. Let  $n_1, n_2, n_3$  be the odd numbers of dotted edges in every cycle, therefore  $n_1 + n_2 + n_3$  is odd. On the other hand, every dotted edge enters twice, so  $n_1 + n_2 + n_3$  is even.

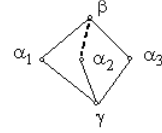


Figure 2.13.

2) Let there exist a root  $\gamma$  connected to all vertices of the square. Then we have 5 cycles:

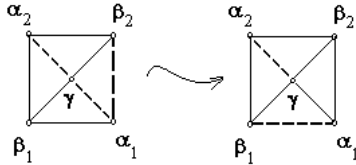


Figure 2.14.

four triangles  $\{\alpha_i, \beta_j, \gamma\}$ , where  $i = 1, 2; j = 1, 2$ , and the square  $\{\alpha_1, \beta_1, \alpha_2, \beta_2\}$ . Every cycle should contain an odd number of dotted edges. Let  $n_1, n_2, n_3, n_4, n_5$  be odd numbers of dotted edges in every cycle, therefore  $n_1 + n_2 + n_3 + n_4 + n_5$  is odd. On the other hand, every dotted edge is entered twice, so  $n_1 + n_2 + n_3 + n_4 + n_5$  is even. For example, the left square is transformed to the right one by the reflection  $s_{\alpha_1}$ ,

see Fig. 2.14. The right square contains the cycle  $\{\alpha_1, \beta_2, \gamma\}$  with 3 solid edges, i.e., the extended Dynkin diagram  $\tilde{A}_2$ , contradicting Proposition A.2. □

**2.3. Classification of simply-laced Carter diagrams with cycles.** The classification of simply-laced Carter diagrams with cycles is based on the following statements:

- (i) the diagram containing any non-Dynkin diagram (in particular, any extended Dynkin diagram) is not a Carter diagram (Proposition 2.1).
- (ii) the diagram containing two cycles with intersection of length  $> 1$  is not a Carter diagram (Proposition 2.3, heading 1)).
- (iii) the diagram which can be equivalently transformed to the diagram of types (i) or (ii) is not a Carter diagram. We use this fact in Lemma 2.5.
- (iv) the Carter diagrams containing cycles of length  $> 4$  can be excluded from Carter's list (Theorem 3.1).

**2.3.1. The Carter diagrams with cycles on 6 vertices.** There are only four 6-vertex simply-laced Carter diagrams containing cycles, see Table 2.3,  $n = 6$ . As we show in Section 3.2, the diagram  $D_6(b_2)$  is equivalent to  $D_6(a_2)$ , so  $D_6(b_2)$  is excluded from the list of Carter diagrams. The diagrams


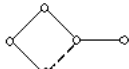
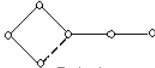
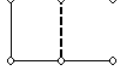

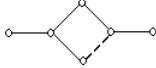

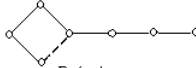
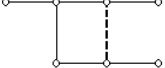
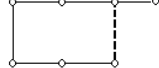
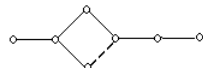
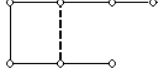
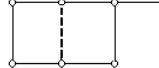

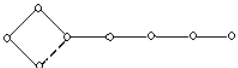
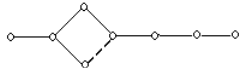
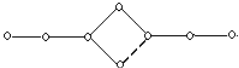
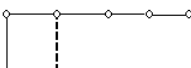

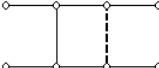


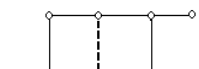
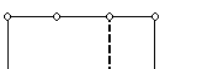
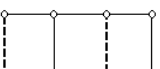
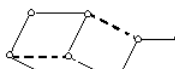

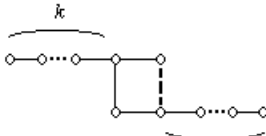
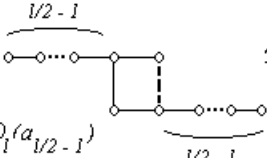
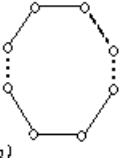
$l$	The Carter diagrams
4-5	 $D_4(a_1)$  $D_5(a_1)$
6	 $D_6(a_1)$  $E_6(a_1)$  $E_6(a_2)$  $D_6(a_2)$ $\simeq$  $D_6(b_2)$
7	 $D_7(a_1)$  $E_7(a_2)$ $\simeq$  $E_7(b_2)$  $D_7(a_2)$  $E_7(a_1)$  $E_7(a_3)$  $E_7(a_4)$
8	 $D_8(a_1)$  $D_8(a_2)$  $D_8(a_3)$  $E_8(a_1)$  $E_8(a_2)$  $E_8(a_3)$ $\simeq$  $E_8(b_3)$  $E_8(a_4)$  $E_8(a_5)$ $\simeq$  $E_8(b_5)$  $E_8(a_6)$  $E_8(a_7)$  $E_8(a_8)$
$l > 8$	 $D_l(a_k)$ $k = 1, 2, \dots, l/2 - 1$  $D_l(a_{l/2-1})$ $\simeq$  $D_l(b_{l/2-1})$ $(l - \text{even})$

Table 2.3. The simply-laced Carter diagrams with cycles

depicted in Fig. 2.15 are not Carter diagrams. One should discard the bold vertex and apply Proposition 2.3, heading 2).



Figure 2.15. Not Carter diagrams on 6-vertices

2.3.2. *The Carter diagrams with cycles on 7 vertices.* There are only six 7-vertex simply-laced Carter diagrams containing cycles, see Table 2.3,  $n = 7$ . According to Section 3.2, the diagram  $E_7(b_2)$  is equivalent to  $E_7(a_2)$ . Thus the diagram  $E_7(b_2)$  is excluded from the list of Carter diagrams. Note that the diagrams (a) and (b) depicted in Fig. 2.16 are not Carter diagrams since each of them contains the extended Dynkin diagram  $\tilde{D}_4$ . The diagrams (c) and (d) are not Carter diagrams since for each of them there exist two cycles with the intersection of length  $> 1$ , see Proposition 2.3. In order to see that (e) and (f) are not Carter diagrams, one can discard bold vertices and apply Proposition 2.3, heading 2).

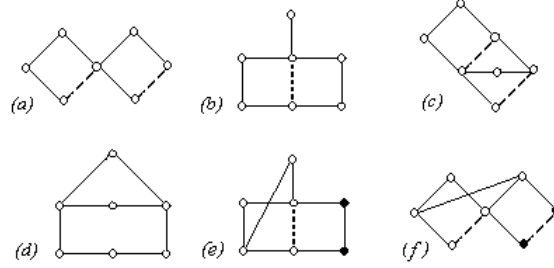


Figure 2.16.

2.3.3. *The Carter diagrams with cycles on 8 vertices.* There are only eleven 8-vertex simply-laced Carter diagrams containing cycles, see Table 2.3,  $n = 8$ .

The diagrams depicted in Fig. 2.17 are not Carter diagrams. One can discard the bold vertices to see that each of depicted diagrams contains an extended Dynkin diagram. The diagram (a) contains  $\tilde{E}_6$ ; (b) and (c) contain  $\tilde{D}_5$ ; (d) and (e) contain  $\tilde{D}_6$ . For diagrams (f) and (g), see Lemma 2.5. The diagram (h) is not a Carter diagram since the intersection of two cycles is of length  $> 1$ , see Proposition 2.3<sup>1</sup>.

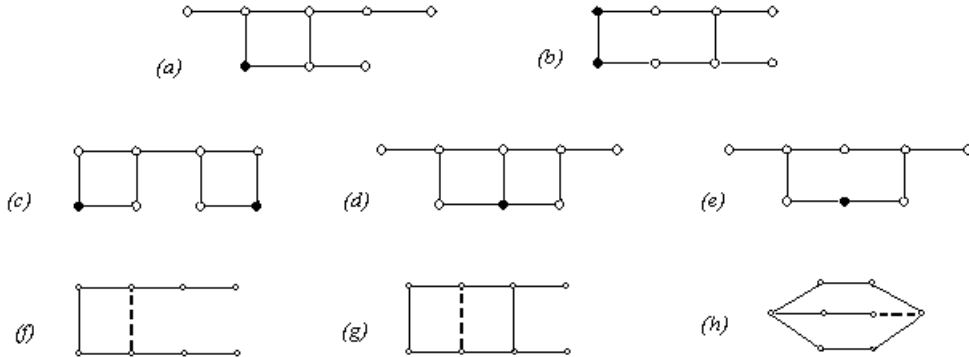


Figure 2.17. 8-vertex diagrams are not Carter diagrams

<sup>1</sup>We do not depict here diagrams corresponding to heading 2) of Proposition 2.3, see Fig. 2.9. For  $l = 6$ , they are depicted in Fig. 2.15, for  $l = 7$ , see diagrams (e), (f) from Section 2.3.2.

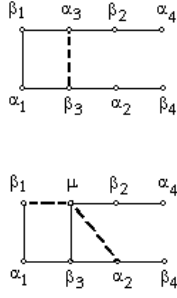


Figure 2.18.

**Lemma 2.5.** *Diagrams (f) and (g) in Fig. 2.17 are not Carter diagrams.*

*Proof.* In cases (f) and (g), we transform the given diagram to an equivalent one containing an extended Dynkin diagram. Consider the diagram (f). The corresponding roots are depicted in the upper diagram in Fig. 2.18. Let  $w$  be the primitive element associated with this diagram:

$$w = s_{\alpha_1} s_{\alpha_2} s_{\alpha_3} s_{\alpha_4} s_{\beta_1} s_{\beta_2} s_{\beta_3} s_{\beta_4}.$$

Since  $s_{\alpha_3} s_{\beta_1} s_{\beta_3} = s_{\beta_1} s_{\beta_3} s_{\mu}$ , where  $\mu = \alpha_3 - \beta_3 + \beta_1$ , we have

$$w = s_{\alpha_1} s_{\alpha_2} s_{\alpha_4} s_{\beta_1} s_{\beta_3} s_{\mu} s_{\beta_2} s_{\beta_4}.$$

Then the element  $w$  is associated with the connection diagram depicted in the lower diagram in Fig. 2.18. Discard the vertex  $\beta_3$ , the remaining diagram is the extended Dynkin diagram  $\tilde{E}_6$ .

Consider the diagram (g) in Fig. 2.17. The corresponding roots are depicted in Fig. 2.19,(1).

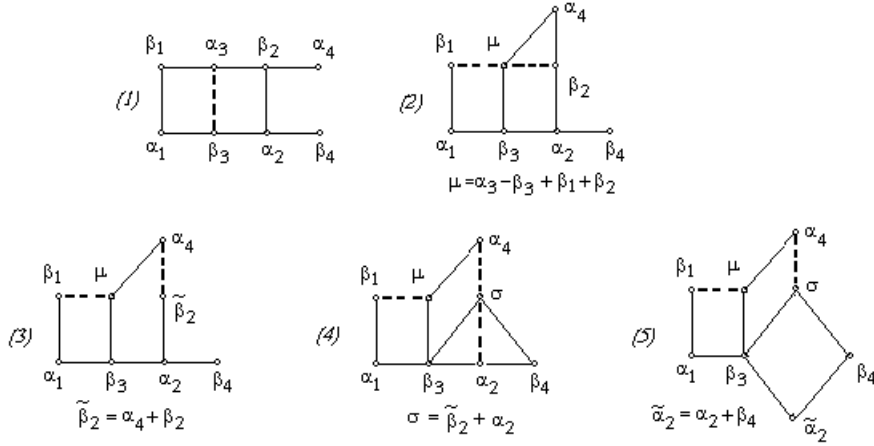


Figure 2.19. The equivalent transformation of diagram (1) to non-Carter diagram (5)

The primitive element associated with the diagram is

$$w = s_{\alpha_1} s_{\alpha_2} s_{\alpha_3} s_{\alpha_4} s_{\beta_1} s_{\beta_2} s_{\beta_3} s_{\beta_4} = s_{\alpha_1} s_{\alpha_2} s_{\alpha_4} (s_{\alpha_3} s_{\beta_1} s_{\beta_2} s_{\beta_3}) s_{\beta_4} = s_{\alpha_1} s_{\alpha_2} s_{\alpha_4} s_{\beta_1} s_{\beta_2} s_{\beta_3} s_{\mu} s_{\beta_4}, \text{ where } \mu = \alpha_3 - \beta_3 + \beta_1 + \beta_2.$$

The last expression of  $w$  is associated with the diagram (2) in Fig. 2.19. The diagram (2) is a connection diagram, but it is not a Carter diagram. Further,

$$w = s_{\alpha_1} s_{\alpha_2} (s_{\alpha_4} s_{\beta_2}) s_{\beta_1} s_{\beta_3} s_{\mu} s_{\beta_4} = s_{\alpha_1} s_{\alpha_2} s_{\tilde{\beta}_2} s_{\alpha_4} s_{\beta_1} s_{\beta_3} s_{\mu} s_{\beta_4}, \text{ where } \tilde{\beta}_2 = \alpha_4 + \beta_2,$$

The obtained expression of  $w$  is associated with the diagram (3) in Fig. 2.19. Further, since  $\beta_4$  is orthogonal to every root depicted in the diagram (3) except for  $\alpha_2$ , we have:

$$w = s_{\alpha_1} (s_{\alpha_2} s_{\tilde{\beta}_2}) s_{\alpha_4} s_{\beta_1} s_{\beta_3} s_{\mu} s_{\beta_4} = s_{\alpha_1} s_{\sigma} (s_{\alpha_2} s_{\beta_4}) s_{\alpha_4} s_{\beta_1} s_{\beta_3} s_{\mu}, \text{ where } \sigma = \tilde{\beta}_2 + \alpha_2.$$

The latter expression of  $w$  is associated with the diagram (4) in Fig. 2.19. Finally,

$$w = s_{\alpha_1} s_{\sigma} s_{\beta_4} s_{\tilde{\alpha}_2} s_{\alpha_4} s_{\beta_1} s_{\beta_3} s_{\mu}, \text{ where } \tilde{\alpha}_2 = \alpha_2 + \beta_4.$$

The element  $w$  is associated with the diagram (5) in Fig. 2.19. The diagram (5) is not a Carter diagram since contains subdiagram  $\{\mu, \sigma, \tilde{\alpha}_2, \alpha_1, \beta_3\}$  that is the diagram  $\tilde{D}_4$ .  $\square$

2.3.4. *The Carter diagrams with cycles on  $l > 8$  vertices.* The Dynkin diagram  $A_n$  does not contain any Carter diagrams with cycles, see Section A.2.2. For the Dynkin diagram  $D_n$ , we refer to Carter's discussion in [Ca72, p. 13]. In this case, there are 2 types of Carter diagrams (Table 2.3,  $l > 8$ ):

- (a) pure cycles  $D_l(b_{\frac{l}{2}-1})$  for  $l$  even,  $l \leq n$
- (b)  $D_l(a_1), D_l(a_2), \dots, D_l(a_{\frac{l}{2}-1})$  for  $l$  - even,  $l \leq n$ .

In Section 3.4, we will show that any pure cycle  $D_l(b_{\frac{l}{2}-1})$  from (a) is equivalent to  $D_l(a_{\frac{l}{2}-1})$  from (b). Thus pure cycles  $D_l(b_{\frac{l}{2}-1})$  can be excluded from Carter's list.

### 3. Exclusion of $n$ -cycles, $n > 4$

In this section, we show that Carter diagrams containing cycles of length  $n > 4$  can be discarded from the list.

**Theorem 3.1.** *Any Carter diagram containing  $l$ -cycles ( $l > 4$ ) is equivalent to another Carter diagram containing only 4-cycles.*

In all cases we construct a certain explicit transformation of the diagram containing  $l$ -cycles ( $l > 4$ ) to a diagram containing only 4-cycles. The corresponding pairs of equivalent diagrams are depicted in Table 3.4.

Note that the coincidence of characteristic polynomials of diagrams in pairs of Table 3.4 is the necessary condition of the equivalence of these diagrams, see Remark 1.5. As it is shown in Theorem 3.1, this condition is also sufficient in the class of Carter diagrams.

For convenience, we consider the pair  $\{D_6(b_2), D_6(b_2)\}$  as a separated case, though this is a particular case of the pair  $\{D_l(b_{\frac{l}{2}-1}), D_l(a_{\frac{l}{2}-1})\}$  with  $l = 6$ , Table 3.4. The idea of explicit transformation connecting elements of every pair is similar for all pairs<sup>1</sup>.

**3.1. The pair of equivalent diagrams  $\{E_8(b_3), E_8(a_3)\}$ .** The element  $w$  associated with the Carter diagram  $E_8(a_3)$  is transformed as follows:

$$\begin{aligned} w &= s_{\alpha_1} s_{\alpha_2} s_{\alpha_3} s_{\alpha_4} s_{\beta_1} s_{\beta_2} s_{\beta_3} s_{\beta_4} = \\ &= s_{\alpha_1} s_{\alpha_4} (s_{\alpha_2} s_{\alpha_3} s_{\beta_3}) s_{\beta_1} s_{\beta_2} s_{\beta_4} = \\ &= s_{\alpha_1} s_{\alpha_4} s_{\mu} s_{\alpha_2} s_{\alpha_3} s_{\beta_1} s_{\beta_2} s_{\beta_4}, \text{ where } \mu = \beta_3 + \alpha_3 - \alpha_2. \end{aligned} \quad (3.1)$$

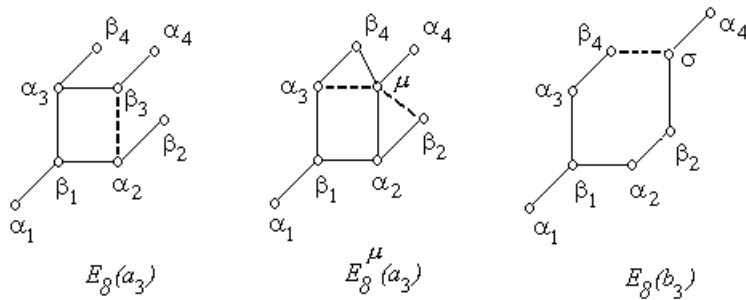


Figure 3.20. The pair  $\{E_8(b_3), E_8(a_3)\}$

From (3.1) we have:

$$\begin{aligned} w &\stackrel{s_{\beta_2} s_{\beta_4}}{\simeq} s_{\alpha_1} s_{\alpha_4} (s_{\beta_2} s_{\beta_4} s_{\mu}) s_{\alpha_2} s_{\alpha_3} s_{\beta_1} = \\ &= s_{\alpha_1} s_{\alpha_4} s_{\sigma} s_{\beta_2} s_{\beta_4} s_{\alpha_2} s_{\alpha_3} s_{\beta_1}, \text{ where } \sigma = \mu - \beta_2 + \beta_4. \end{aligned} \quad (3.2)$$

<sup>1</sup>Perhaps redrawing elements of pairs as the projection of 3-dimensional cube in Fig. 3.20 – Fig. 3.26 may give a hint to the geometric interpretation of these explicit transformations.



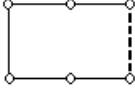
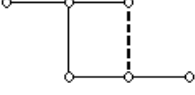
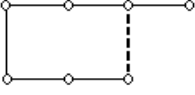
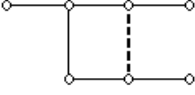
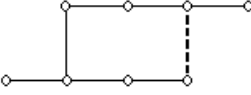
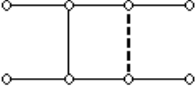
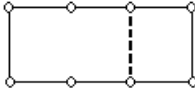
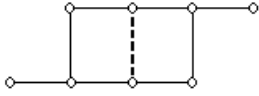
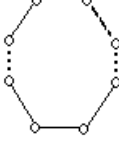
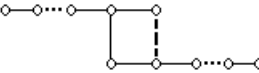
	The Carter diagram with $n$ -cycles, $n > 4$	The equivalent Carter diagram, only 4-cycles	The characteristic polynomial of the primitive element
1	 $D_6(b_2), n = 6$	 $D_6(a_2)$	$(t^3 + 1)^2$
2	 $E_7(b_2), n = 6$	 $E_7(a_2)$	$(t^4 - t^2 + 1)(t^2 - t + 1)(t + 1)$
3	 $E_8(b_3), n = 6$	 $E_8(a_3)$	$(t^4 - t^2 + 1)^2$
4	 $E_8(b_5), n = 6$	 $E_8(a_5)$	$t^8 - t^7 + t^5 - t^4 + t^3 - t^2 + 1$
5	 $D_l(b_{\frac{1}{2}l-1}), n = l, (l - \text{even})$	 $D_l(a_{\frac{1}{2}l-1}), n = l, (l - \text{even})$	$(t^{\frac{l}{2}} + 1)^2$

Table 3.4. Pairs of equivalent Carter diagrams

So,  $\sigma = \beta_3 + \alpha_3 - \alpha_2 - \beta_2 + \beta_4$ , and it is easy to see that

$$\begin{aligned}
 (\sigma, \alpha_3) &= (\alpha_3, \alpha_3) + (\alpha_3, \beta_4) + (\alpha_3, \beta_3) = 1 - \frac{1}{2} - \frac{1}{2} = 0, \\
 (\sigma, \alpha_2) &= -(\alpha_2, \alpha_2) - (\alpha_2, \beta_2) + (\alpha_2, \beta_3) = -1 + \frac{1}{2} + \frac{1}{2} = 0, \\
 (\sigma, \beta_1) &= -(\alpha_2, \beta_1) + (\alpha_3, \beta_1) = \frac{1}{2} - \frac{1}{2} = 0, \\
 (\sigma, \alpha_1) &= 0, \\
 (\sigma, \beta_4) &= (\beta_4, \beta_4) + (\alpha_3, \beta_4) = 1 - \frac{1}{2} = \frac{1}{2}, \\
 (\sigma, \beta_2) &= -(\beta_2, \beta_2) - (\alpha_2, \beta_2) = -1 + \frac{1}{2} = -\frac{1}{2}, \\
 (\sigma, \alpha_4) &= (\beta_3, \alpha_4) = -\frac{1}{2}.
 \end{aligned} \tag{3.3}$$

Relations (3.3) describe the Carter diagram  $E_8(b_3)$ , Fig. 3.20. We only need to check that the element  $w$  is expressed as a product of two involutions:

$$\begin{aligned}
 w = s_{\alpha_1} s_{\alpha_4} s_{\sigma} s_{\beta_2} s_{\beta_4} s_{\alpha_2} s_{\alpha_3} s_{\beta_1} &\stackrel{s_{\alpha_4}}{\simeq} s_{\alpha_1} s_{\sigma} (s_{\beta_2} s_{\beta_4} s_{\alpha_4}) s_{\alpha_2} s_{\alpha_3} s_{\beta_1} \stackrel{s_{\sigma}}{\simeq} \\
 s_{\alpha_1} (s_{\beta_2} s_{\beta_4} s_{\alpha_4}) (s_{\alpha_2} s_{\alpha_3} s_{\sigma}) s_{\beta_1} &= (s_{\beta_2} s_{\beta_4} s_{\alpha_4}) (s_{\alpha_1} s_{\alpha_2} s_{\alpha_3} s_{\sigma}) s_{\beta_1} \stackrel{s_{\beta_1}}{\simeq} \\
 (s_{\beta_1} s_{\beta_2} s_{\beta_4} s_{\alpha_4}) (s_{\alpha_1} s_{\alpha_2} s_{\alpha_3} s_{\sigma}). &
 \end{aligned} \tag{3.4}$$

Thus,  $w_1 = s_{\beta_1} s_{\beta_2} s_{\beta_4} s_{\alpha_4}$ ,  $w_2 = s_{\alpha_1} s_{\alpha_2} s_{\alpha_3} s_{\sigma}$  are two involutions,  $w = w_1 w_2$  and  $w$  is associated with diagram  $E_8(b_3)$ , which was to be proven.

**3.2. The pair of equivalent diagrams  $\{E_7(b_2), E_7(a_2)\}$  and  $\{D_6(b_2), D_6(a_2)\}$ .** These cases directly follow from the case  $(E_8(b_3), E_8(a_3))$  that we see from Fig. 3.21 and Fig. 3.22.

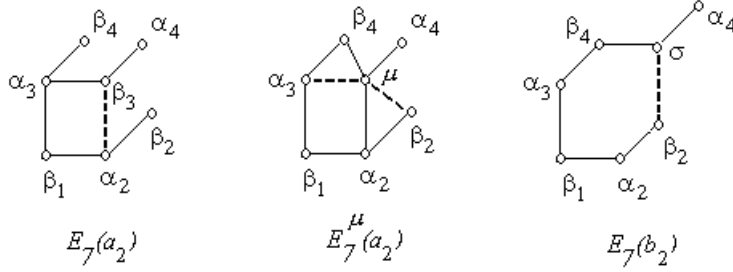


Figure 3.21. The pair  $\{E_7(b_2), E_7(a_2)\}$

For the case  $\{E_7(b_2), E_7(a_2)\}$ , we discard  $s_{\alpha_1}$  in relations (3.1)-(3.4) as follows:

$$\begin{aligned}
 w = s_{\alpha_2} s_{\alpha_3} s_{\alpha_4} s_{\beta_1} s_{\beta_2} s_{\beta_3} s_{\beta_4} &= \\
 s_{\alpha_4} s_{\mu} s_{\alpha_2} s_{\alpha_3} s_{\beta_1} s_{\beta_2} s_{\beta_4} \text{ (where } \mu = \beta_3 + \alpha_3 - \alpha_2) &\stackrel{s_{\beta_2} s_{\beta_4}}{\simeq} \\
 s_{\alpha_4} s_{\sigma} s_{\beta_2} s_{\beta_4} s_{\alpha_2} s_{\alpha_3} s_{\beta_1} \text{ (where } \sigma = \mu - \beta_2 + \beta_4) &\stackrel{s_{\alpha_4}}{\simeq} \\
 s_{\sigma} (s_{\beta_2} s_{\beta_4} s_{\alpha_4}) s_{\alpha_2} s_{\alpha_3} s_{\beta_1} &\stackrel{s_{\sigma}}{\simeq} (s_{\beta_2} s_{\beta_4} s_{\alpha_4}) (s_{\alpha_2} s_{\alpha_3} s_{\sigma}) s_{\beta_1} \stackrel{s_{\beta_1}}{\simeq} \\
 (s_{\beta_1} s_{\beta_2} s_{\beta_4} s_{\alpha_4}) (s_{\alpha_2} s_{\alpha_3} s_{\sigma}). &
 \end{aligned} \tag{3.5}$$

Here,  $w_1 = s_{\beta_1} s_{\beta_2} s_{\beta_4} s_{\alpha_4}$  and  $w_2 = s_{\alpha_2} s_{\alpha_3} s_{\sigma}$  are two involutions,  $w = w_1 w_2$  and  $w$  is associated with the diagram  $E_7(b_2)$ , which was to be proven. For the case  $(D_6(b_2), D_6(a_2))$ , we discard  $s_{\alpha_4}$  in relation (3.5):

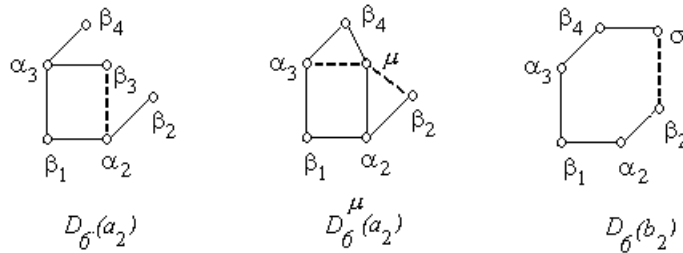


Figure 3.22. The pair  $\{D_6(b_2), D_6(a_2)\}$

$$\begin{aligned}
w &= s_{\alpha_2} s_{\alpha_3} s_{\beta_1} s_{\beta_2} s_{\beta_3} s_{\beta_4} = \\
& s_{\mu} s_{\alpha_2} s_{\alpha_3} s_{\beta_1} s_{\beta_2} s_{\beta_4} \quad (\text{where } \mu = \beta_3 + \alpha_3 - \alpha_2) \stackrel{s_{\beta_2} s_{\beta_4}}{\simeq} \\
& s_{\sigma} s_{\beta_2} s_{\beta_4} s_{\alpha_2} s_{\alpha_3} s_{\beta_1} \quad (\text{where } \sigma = \mu - \beta_2 + \beta_4) \stackrel{s_{\sigma}}{\simeq} (s_{\beta_2} s_{\beta_4})(s_{\alpha_2} s_{\alpha_3} s_{\sigma}) s_{\beta_1} \stackrel{s_{\beta_1}}{\simeq} \\
& (s_{\beta_1} s_{\beta_2} s_{\beta_4})(s_{\alpha_2} s_{\alpha_3} s_{\sigma}).
\end{aligned} \tag{3.6}$$

Here,  $w_1 = s_{\beta_1} s_{\beta_2} s_{\beta_4}$  and  $w_2 = s_{\alpha_2} s_{\alpha_3} s_{\sigma}$  are two involutions,  $w = w_1 w_2$  and  $w$  is associated with diagram  $E_7(b_2)$ .

**3.3. The pair of equivalent diagrams  $\{E_8(b_5), E_8(a_5)\}$ .** This case is the most difficult.

*Step 1.* Let us transform the element  $w$  associated with the Carter diagram  $E_8(b_5)$  as follows:

$$\begin{aligned}
w &= (s_{\beta_1} s_{\beta_2} s_{\beta_4} s_{\gamma})(s_{\alpha_1} s_{\alpha_2} s_{\alpha_3} s_{\alpha_4}) \stackrel{s_{\alpha_4}}{\simeq} s_{\alpha_4} s_{\beta_2} s_{\beta_4} (s_{\beta_1} s_{\gamma} s_{\alpha_1} s_{\alpha_2} s_{\alpha_3}) = \\
& (s_{\beta_2} s_{\beta_4} s_{\mu})(s_{\beta_1} s_{\gamma} s_{\alpha_1} s_{\alpha_2} s_{\alpha_3}), \quad \text{where } \mu = \alpha_4 - \beta_2 + \beta_4.
\end{aligned} \tag{3.7}$$

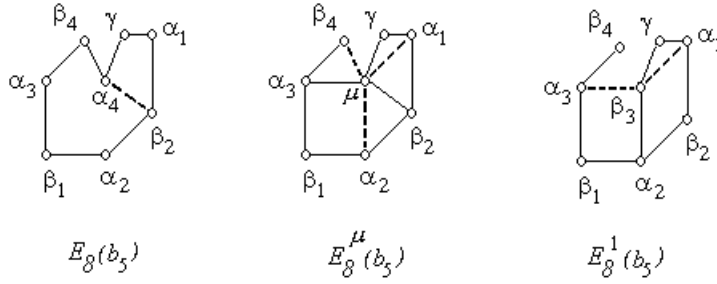


Figure 3.23. Transformation of  $E_8(b_5)$ , step 1

We have

$$\begin{aligned}
(\mu, \alpha_3) &= (\beta_4, \alpha_3) = -\frac{1}{2}, & (\mu, \beta_4) &= (\beta_4, \beta_4) + (\beta_4, \alpha_4) = 1 - \frac{1}{2} = \frac{1}{2}, \\
(\mu, \alpha_2) &= -(\beta_2, \alpha_2) = \frac{1}{2}, & (\mu, \beta_2) &= -(\beta_2, \beta_2) + (\alpha_4, \beta_2) = -1 + \frac{1}{2} = -\frac{1}{2}, \\
(\mu, \alpha_1) &= -(\beta_2, \alpha_1) = \frac{1}{2}.
\end{aligned}$$

see  $E_8^\mu(b_5)$  in Fig. 3.23.

Further,

$$\begin{aligned}
w &= (s_{\beta_2} s_{\beta_4} s_{\beta_1}) s_{\mu} s_{\alpha_2} s_{\alpha_3} (s_{\gamma} s_{\alpha_1}) = \\
& (s_{\beta_2} s_{\beta_4} s_{\beta_1})(s_{\alpha_2} s_{\alpha_3} s_{\beta_3})(s_{\gamma} s_{\alpha_1}), \quad \text{where } \beta_3 = \mu - \alpha_2 + \alpha_3.
\end{aligned} \tag{3.8}$$

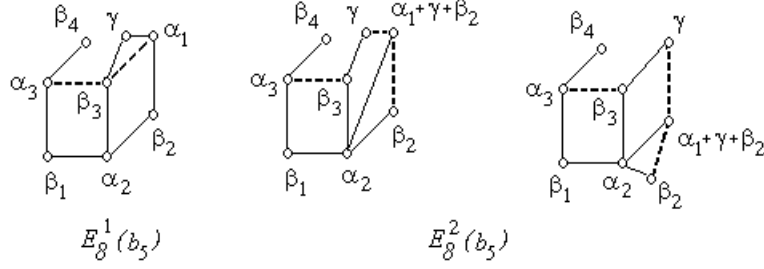
Here,

$$\begin{aligned}
(\beta_3, \alpha_3) &= (\mu, \alpha_3) + (\alpha_3, \alpha_3) = -\frac{1}{2} + 1 = \frac{1}{2}, & (\beta_3, \beta_4) &= (\mu, \beta_4) + (\alpha_3, \beta_4) = \frac{1}{2} - \frac{1}{2} = 0, \\
(\beta_3, \alpha_2) &= (\mu, \alpha_2) - (\alpha_2, \alpha_2) = \frac{1}{2} - 1 = -\frac{1}{2}, & (\beta_3, \beta_2) &= (\mu, \beta_2) - (\alpha_2, \beta_2) = \frac{1}{2} - \frac{1}{2} = 0,
\end{aligned}$$

see  $E_8^1(b_5)$  in Fig. 3.23.

*Step 2.* From (3.8),

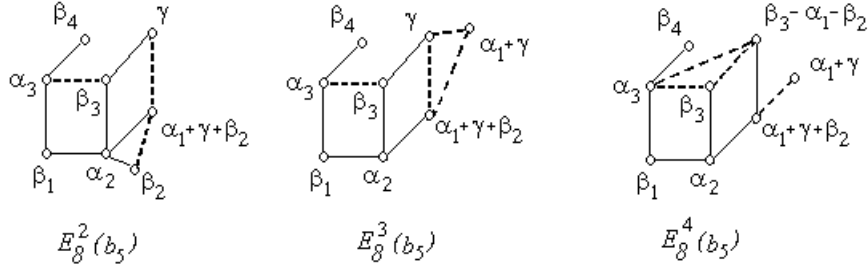
$$\begin{aligned}
w &\stackrel{s_{\beta_2} s_{\beta_4} s_{\beta_1}}{\simeq} s_{\alpha_2} s_{\alpha_3} s_{\beta_3} (s_{\alpha_1 + \gamma} s_{\gamma}) s_{\beta_2} s_{\beta_4} s_{\beta_1} = \\
& \alpha_2 s_{\alpha_3} s_{\beta_3} s_{\alpha_1 + \gamma} (s_{\beta_2} s_{\beta_4} s_{\beta_1}) s_{\gamma} = s_{\alpha_2} s_{\alpha_3} (s_{\beta_3} s_{\beta_2} s_{\beta_4} s_{\beta_1}) s_{\alpha_1 + \gamma + \beta_2} s_{\gamma} \stackrel{s_{\alpha_2} s_{\alpha_3}}{\simeq} \\
& (s_{\beta_3} s_{\beta_2} s_{\beta_4} s_{\beta_1}) s_{\alpha_1 + \gamma + \beta_2} s_{\alpha_2} s_{\alpha_3} s_{\gamma} = s_{\beta_2} (s_{\beta_1} s_{\beta_3} s_{\beta_4} s_{\alpha_1 + \gamma + \beta_2}) (s_{\alpha_2} s_{\alpha_3} s_{\gamma}),
\end{aligned} \tag{3.9}$$

Figure 3.24. Transformation of  $E_8(b_5)$ , step 2

where

$$\begin{aligned}
 (\alpha_1 + \gamma + \beta_2, \beta_3) &= (\beta_3, \alpha_1) + (\beta_3, \gamma) = \frac{1}{2} - \frac{1}{2} = 0, \\
 (\alpha_1 + \gamma + \beta_2, \gamma) &= (\gamma, \gamma) + (\gamma, \alpha_1) = 1 - \frac{1}{2} = \frac{1}{2}, \\
 (\alpha_1 + \gamma + \beta_2, \alpha_2) &= (\beta_2, \alpha_2) = -\frac{1}{2}, \\
 (\alpha_1 + \gamma + \beta_2, \beta_2) &= (\beta_2, \beta_2) + (\beta_2, \alpha_1) = 1 - \frac{1}{2} = \frac{1}{2},
 \end{aligned}$$

see  $E_8^2(b_5)$  in Fig. 3.24.

Figure 3.25. Transformations from  $E_8^2(b_5)$  to  $E_8^3(b_5)$  and from  $E_8^3(b_5)$  to  $E_8^4(b_5)$ 

*Step 3.* Let us transform the element  $w$  from (3.9) (associated with the connection diagram  $E_8^2(b_5)$ , see Fig. 3.25) to a certain element associated with diagram  $E_8^3(b_5)$ . Of course, all our transformations are performed in the conjugacy class of  $w$ .

$$\begin{aligned}
 w &= s_{\beta_2}(s_{\beta_1}s_{\beta_3}s_{\beta_4}s_{\alpha_1+\gamma+\beta_2})(s_{\alpha_2}s_{\alpha_3}s_{\gamma}) = \\
 &= (s_{\beta_1}s_{\beta_3}s_{\beta_4})(s_{\beta_2}s_{\alpha_1+\gamma+\beta_2})(s_{\alpha_2}s_{\alpha_3}s_{\gamma}) = (s_{\beta_1}s_{\beta_3}s_{\beta_4})(s_{\alpha_1+\gamma+\beta_2}s_{\alpha_1+\gamma})(s_{\alpha_2}s_{\alpha_3}s_{\gamma}),
 \end{aligned} \tag{3.10}$$

where

$$\begin{aligned}
 (\alpha_1 + \gamma, \alpha_2) &= (\alpha_1 + \gamma + \beta_2, \alpha_2) - (\beta_2, \alpha_2) = -\frac{1}{2} + (\beta_2, \alpha_2) = 0, \\
 (\alpha_1 + \gamma, \tau) &= (\alpha_1 + \gamma + \beta_2, \tau) - (\beta_2, \tau) = 0 \text{ for } \tau = \beta_1, \beta_3, \beta_4, \alpha_3, \\
 (\alpha_1 + \gamma, \gamma) &= -\frac{1}{2} + 1 = \frac{1}{2}.
 \end{aligned}$$

*Step 4.* Now, we transform the element  $w$  from (3.10) (associated with the connection diagram  $E_8^3(b_5)$ , see Fig. 3.25) to a certain element associated with the connection diagram  $E_8^4(b_5)$ .

$$\begin{aligned}
 w &= (s_{\beta_1}s_{\beta_3}s_{\beta_4})(s_{\alpha_1+\gamma+\beta_2}s_{\alpha_1+\gamma})(s_{\alpha_2}s_{\alpha_3}s_{\gamma}) \stackrel{s_{\gamma}}{\simeq} \\
 &= s_{\gamma}s_{\beta_3}s_{\alpha_1+\gamma+\beta_2}(s_{\beta_1}s_{\beta_4})s_{\alpha_1+\gamma}(s_{\alpha_2}s_{\alpha_3}) = s_{\beta_3}s_{\alpha_1+\gamma+\beta_2}s_{\beta_3-\alpha_1-\beta_2}s_{\alpha_1+\gamma}s_{\beta_1}s_{\beta_4}(s_{\alpha_2}s_{\alpha_3}),
 \end{aligned} \tag{3.11}$$

since  $\beta_3 - \alpha_1 - \beta_2 = \gamma + \beta_3 - (\alpha_1 + \gamma + \beta_2)$ , and  $s_{\gamma}s_{\beta_3}s_{\alpha_1+\gamma+\beta_2} = s_{\beta_3}s_{\alpha_1+\gamma+\beta_2}s_{\beta_3-\alpha_1-\beta_2}$ .



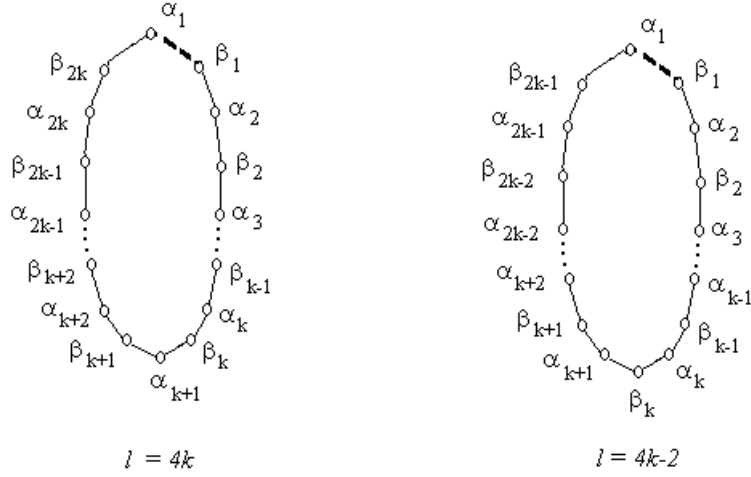


Figure 3.27. Two cases of even cycles  $D_l(b_{\frac{l}{2}-1})$ : 1)  $l = 4k$ ; 2)  $l = 4k - 2$

*Case 2).*  $l = 4k - 2$ . The opposite vertices, i.e., vertices at distance  $2k - 1$ , are of the different types, for example,  $\alpha_1$  and  $\beta_k$ , see Fig. 3.27[right].

3.4.1. *The case  $l = 4k$ .* Let us consider the chains of vertices passing through the top vertex  $\alpha_1$  and with endpoints lying on the same horizontal level, see Fig. 3.27. Let  $L$  (resp.  $R$ ) be the index of the left (resp. right) end of the chain. Then the endpoints of these chains are as follows:

$$\begin{aligned} \{\beta_L, \beta_R\}, \quad L = 2k - i + 1, R = i, \quad 1 \leq i \leq k, \text{ or} \\ \{\alpha_L, \alpha_R\}, \quad L = 2k - i + 2, R = i, \quad 2 \leq i \leq k. \end{aligned} \quad (3.13)$$

Let us consider the following vectors associated with chains (3.13):

$$\begin{aligned} \theta(\beta_L, \beta_R) &= \alpha_1 - \sum_{i=1}^R \beta_i - \sum_{i=2}^R \alpha_i + \sum_{i=L}^{2k} \beta_i + \sum_{i=L+1}^{2k} \alpha_i, \quad R + L = 2k + 1, \\ \theta(\alpha_L, \alpha_R) &= \alpha_1 - \sum_{i=1}^{R-1} \beta_i - \sum_{i=2}^R \alpha_i + \sum_{i=L}^{2k} \beta_i + \sum_{i=L}^{2k} \alpha_i, \quad R + L = 2k + 2. \end{aligned} \quad (3.14)$$

We have the following actions on vectors (3.14):

$$\begin{aligned} s_{\beta_1} s_{\beta_{2k}} \alpha_1 &= \theta(\beta_1, \beta_{2k}), \\ s_{\alpha_2} s_{\alpha_{2k}} \theta(\beta_1, \beta_{2k}) &= \theta(\alpha_2, \alpha_{2k}), \\ &\dots \\ s_{\beta_{L-1}} s_{\beta_R} \theta(\alpha_L, \alpha_R) &= \theta(\beta_{L-1}, \beta_R), \\ s_{\alpha_L} s_{\alpha_{R+1}} \theta(\beta_L, \beta_R) &= \theta(\alpha_L, \alpha_{R+1}). \end{aligned} \quad (3.15)$$

Thus,  $\theta(\beta_L, \beta_R)$ ,  $\theta(\alpha_L, \alpha_R)$  from (3.14) are roots. The following orthogonality relations hold

$$\begin{aligned} \theta(\beta_L, \beta_R) &\perp \beta_i, i \neq R, L, \quad \theta(\beta_L, \beta_R) \not\perp \beta_L, \beta_R, \\ \theta(\beta_L, \beta_R) &\perp \alpha_i, i \neq R + 1, L, \quad \theta(\beta_L, \beta_R) \not\perp \alpha_{R+1}, \alpha_L (R \neq k), \quad \theta(\beta_{k+1}, \beta_k) \perp \alpha_{k+1}, \\ \theta(\alpha_L, \alpha_R) &\perp \beta_i, i \neq L - 1, R, \quad \theta(\alpha_L, \alpha_R) \not\perp \beta_{L-1}, \beta_R, \\ \theta(\alpha_L, \alpha_R) &\perp \alpha_i, i \neq R, L, \quad \theta(\alpha_L, \alpha_R) \not\perp \alpha_L, \alpha_R. \end{aligned} \quad (3.16)$$

**Lemma 3.2.** *The following commutation relations hold:*

$$\begin{aligned} s_{\theta(\beta_L, \beta_R)} \prod_{i=1}^{2k} s_{\alpha_i} &= \left( \prod_{i=1}^{2k} s_{\alpha_i} \right) s_{\theta(\alpha_L, \alpha_{R+1})}, \quad L + R = 2k + 1, \quad R \leq k, \\ s_{\theta(\alpha_L, \alpha_R)} \prod_{i=1}^{2k} s_{\beta_i} &= \left( \prod_{i=1}^{2k} s_{\beta_i} \right) s_{\theta(\beta_{L-1}, \beta_R)}, \quad L + R = 2k + 2, \quad R \leq k. \end{aligned} \quad (3.17)$$

*Proof.* According to the orthogonality relations (3.16), we have

$$\begin{aligned} s_{\theta(\beta_L, \beta_R)} \prod_{i=1}^{2k} s_{\alpha_i} &= \left( \prod_{\alpha_i \neq R+1, L} s_{\alpha_i} \right) s_{\theta(\beta_L, \beta_R)} s_{\alpha_{R+1}} s_{\alpha_L} = \\ &= \left( \prod_{\alpha_i \neq R+1, L} s_{\alpha_i} \right) s_{\alpha_{R+1}} s_{\alpha_L} s_{\theta(\beta_L, \beta_R) - \alpha_{R+1} + \alpha_L} = \left( \prod_{i=1}^{2k} s_{\alpha_i} \right) s_{\theta(\alpha_L, \alpha_{R+1})}. \end{aligned}$$

Similarly,

$$\begin{aligned} s_{\theta(\alpha_L, \alpha_R)} \prod_{i=1}^{2k} s_{\beta_i} &= \left( \prod_{\beta_i \neq R, L-1} s_{\beta_i} \right) s_{\theta(\alpha_L, \alpha_R)} s_{\beta_{L-1}} s_{\beta_R} = \\ &= \left( \prod_{\beta_i \neq R, L-1} s_{\beta_i} \right) s_{\beta_{L-1}} s_{\beta_R} s_{\theta(\alpha_L, \alpha_R) - \beta_R + \beta_{L-1}} = \left( \prod_{i=1}^{2k} s_{\beta_i} \right) s_{\theta(\beta_{L-1}, \beta_R)}. \end{aligned}$$

□

**Proposition 3.3.** *Let*

$$w = w\beta w\alpha = \prod_{i=1}^{2k} s_{\beta_i} \prod_{i=1}^{2k} s_{\alpha_i}$$

*be the element associated with the cycle  $D_l(b_{\frac{1}{2}l-1})$ , where  $l = 4k$ , Fig. 3.27. The element  $w$  is conjugate to the element*

$$\left( \prod_{i=1}^{2k} s_{\beta_i} \right) s_{\theta(\beta_{k+1}, \beta_k)} \left( \prod_{i=2}^{2k} s_{\alpha_i} \right). \quad (3.18)$$

*Proof.* First, we have

$$w = \prod s_{\beta_i} \prod s_{\alpha_j} \stackrel{s_{\alpha_1}}{\simeq} s_{\alpha_1} (s_{\beta_1} s_{\beta_{2k}}) \prod_{i \neq 1, 2k} s_{\beta_i} \prod_{j \neq 1} s_{\alpha_j} = s_{\beta_1} s_{\beta_{2k}} s_{\theta(\beta_{2k}, \beta_1)} \prod_{i \neq 1, 2k} s_{\beta_i} \prod_{j \neq 1} s_{\alpha_j}.$$

By (3.16), the elements  $s_{\theta(\beta_1, \beta_{2k})}$  and  $\prod_{i \neq 1, 2k} s_{\beta_i}$  commute, and we have:

$$w = s_{\beta_1} s_{\beta_{2k}} \left( \prod_{i \neq 1, 2k} s_{\beta_i} \right) s_{\theta(\beta_{2k}, \beta_1)} \prod_{j \neq 1} s_{\alpha_j} = \left( \prod s_{\beta_i} \right) s_{\theta(\beta_{2k}, \beta_1)} \left( \prod s_{\alpha_j} \right).$$

Further, we use Lemma 3.2 as follows:

$$\begin{aligned} w &= \prod s_{\beta_i} \left( \prod s_{\alpha_j} \right) s_{\theta(\alpha_{2k}, \alpha_2)} \stackrel{s_{\theta(\alpha_{2k}, \alpha_2)}}{\simeq} s_{\theta(\alpha_{2k}, \alpha_2)} \prod s_{\beta_i} \prod s_{\alpha_j} = \left( \prod s_{\beta_i} \right) s_{\theta(\beta_{2k-1}, \beta_2)} \prod s_{\alpha_j} = \\ &= \prod s_{\beta_i} \left( \prod s_{\alpha_j} \right) s_{\theta(\alpha_{2k-1}, \alpha_3)} \stackrel{s_{\theta(\alpha_{2k-1}, \alpha_3)}}{\simeq} s_{\theta(\alpha_{2k-1}, \alpha_3)} \prod s_{\beta_i} \prod s_{\alpha_j} = \left( \prod s_{\beta_i} \right) s_{\theta(\beta_{2k-2}, \beta_3)} \prod s_{\alpha_j} = \\ &\dots \\ &= \left( \prod s_{\beta_i} \right) s_{\theta(\beta_{k+1}, \beta_k)} \prod s_{\alpha_j}. \end{aligned}$$

The relation (3.18) is proved. □

**Corollary 3.4.** *The conjugate class containing elements*

$$\prod_{i=1}^{2k} s_{\beta_i} \prod_{i=1}^{2k} s_{\alpha_i} \simeq \left( \prod_{i=1}^{2k} s_{\beta_i} \right) (s_{\theta(\beta_{k+1}, \beta_k)} \prod_{i=2}^{2k} s_{\alpha_i}) \quad (3.19)$$

is associated with both  $D_l(b_{\frac{l}{2}-1})$  and  $D_l(a_{\frac{l}{2}-1})$ , where  $l = 4k$ , Fig. 3.28.

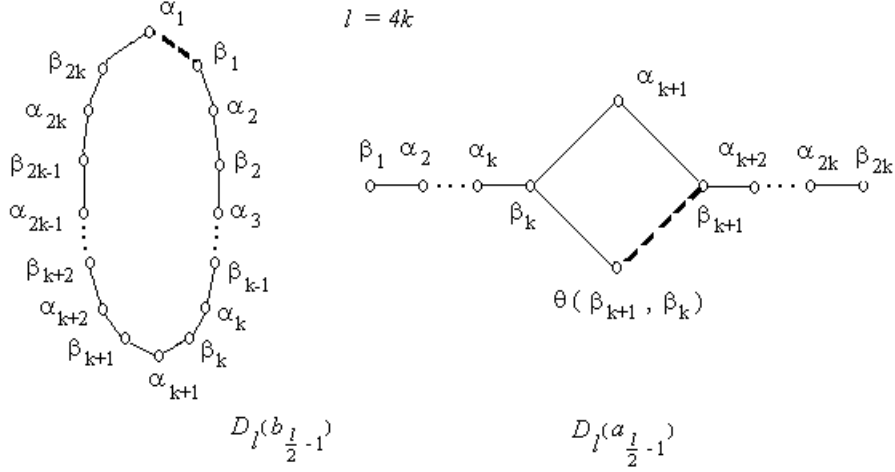


Figure 3.28. The equivalent diagrams  $D_l(b_{\frac{l}{2}-1})$  and  $D_l(a_{\frac{l}{2}-1})$ , where  $l = 4k$

For  $i \neq k+1$ , the orthogonality  $\theta(\beta_{k+1}, \beta_k) \perp \alpha_i$  follows from (3.16). For  $i = k+1$ , it is easy to check:

$$(\theta(\beta_{k+1}, \beta_k), \alpha_{k+1}) = (\beta_{k+1}, \alpha_{k+1}) - (\beta_k, \alpha_{k+1}) = -\frac{1}{2} + \frac{1}{2} = 0.$$

Besides, for  $i \neq k, k+1$ , we have  $\theta(\beta_{k+1}, \beta_k) \perp \beta_i$ , see (3.16). At last, for  $i = k, k+1$ , we have:

$$\begin{aligned} (\theta(\beta_{k+1}, \beta_k), \beta_k) &= (-\beta_k, \beta_k) + (-\alpha_k, \beta_k) = -1 + \frac{1}{2} = -\frac{1}{2}. \\ (\theta(\beta_{k+1}, \beta_k), \beta_{k+1}) &= (\beta_{k+1}, \beta_{k+1}) + (\alpha_{k+2}, \beta_{k+1}) = 1 - \frac{1}{2} = \frac{1}{2}. \quad \square \end{aligned}$$

3.4.2. *The case  $l = 4k - 2$ .* Similarly to (3.13), we consider chains

$$\begin{aligned} \{\beta_L, \beta_R\}, \quad L = 2k - i, R = i, \quad 1 \leq i \leq k-1, \text{ or} \\ \{\alpha_L, \alpha_R\}, \quad L = 2k - i + 1, R = i, \quad 2 \leq i \leq k. \end{aligned} \quad (3.20)$$

Then we consider the following vectors associated with the chains (3.20):

$$\begin{aligned} \mu(\beta_L, \beta_R) &= \alpha_1 - \sum_{i=1}^R \beta_i - \sum_{i=2}^R \alpha_i + \sum_{i=L}^{2k-1} \beta_i + \sum_{i=L+1}^{2k-1} \alpha_i, \quad R + L = 2k, \\ \mu(\alpha_L, \alpha_R) &= \alpha_1 - \sum_{i=1}^{R-1} \beta_i - \sum_{i=2}^R \alpha_i + \sum_{i=L}^{2k-1} \beta_i + \sum_{i=L}^{2k-1} \alpha_i, \quad R + L = 2k + 1. \end{aligned} \quad (3.21)$$

As above,  $\mu(\beta_L, \beta_R), \mu(\alpha_L, \alpha_R)$  from (3.21) are roots.



**Lemma 3.5.** *The following commutation relations hold:*

$$\begin{aligned} s_{\mu(\beta_L, \beta_R)} \prod_{i=1}^{2k-1} s_{\alpha_i} &= \left( \prod_{i=1}^{2k-1} s_{\alpha_i} \right) s_{\mu(\alpha_L, \alpha_{R+1})}, \quad L + R = 2k, \quad R \leq k-1, \\ s_{\mu(\alpha_L, \alpha_R)} \prod_{i=1}^{2k-1} s_{\beta_i} &= \left( \prod_{i=1}^{2k-1} s_{\beta_i} \right) s_{\mu(\beta_{L-1}, \beta_R)}, \quad L + R = 2k+1, \quad R \leq k. \end{aligned} \quad (3.22)$$

In fact, the proof is as in Lemma 3.2.  $\square$

**Proposition 3.6.** *Let*

$$w = w_\beta w_\alpha = \prod_{i=1}^{2k-1} s_{\beta_i} \prod_{i=1}^{2k-1} s_{\alpha_i}$$

*be the element associated with the cycle  $D_l(b_{\frac{1}{2}l-1})$ , where  $l = 4k - 2$ , Fig. 3.27. The element  $w$  is conjugate to the element*

$$s_{\mu(\alpha_{k+1}, \alpha_k)} \left( \prod_{i=1}^{2k-1} s_{\beta_i} \right) \left( \prod_{i=2}^{2k-1} s_{\alpha_i} \right). \quad (3.23)$$

*Proof.* As in Proposition 3.3, we have

$$\begin{aligned} w &= \prod s_{\beta_i} \prod s_{\alpha_j} \stackrel{s_{\alpha_1}}{\simeq} s_{\alpha_1} (s_{\beta_1} s_{\beta_{2k-1}}) \prod_{i \neq 1, 2k-1} s_{\beta_i} \prod_{j \neq 1} s_{\alpha_j} = s_{\beta_1} s_{\beta_{2k-1}} s_{\mu(\beta_{2k-1}, \beta_1)} \prod_{i \neq 1, 2k-1} s_{\beta_i} \prod_{j \neq 1} s_{\alpha_j} = \\ &= s_{\beta_1} s_{\beta_{2k-1}} \left( \prod_{i \neq 1, 2k-1} s_{\beta_i} \right) s_{\mu(\beta_{2k-1}, \beta_1)} \prod_{j \neq 1} s_{\alpha_j} = \left( \prod s_{\beta_i} \right) s_{\mu(\beta_{2k-1}, \beta_1)} \left( \prod_{j \neq 1} s_{\alpha_j} \right). \end{aligned}$$

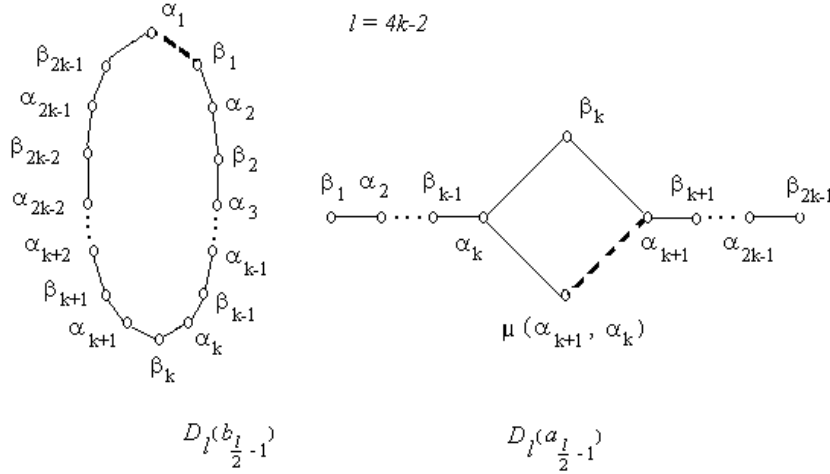


Figure 3.29. The equivalent diagrams  $D_l(b_{\frac{1}{2}l-1})$  and  $D_l(a_{\frac{1}{2}l-1})$ , where  $l = 4k - 2$

By Lemma 3.5, we have:

$$\begin{aligned} w &= \prod s_{\beta_i} \left( \prod_{j \neq 1} s_{\alpha_j} \right) s_{\mu(\alpha_{2k-1}, \alpha_2)} \stackrel{s_{\mu(\alpha_{2k-1}, \alpha_2)}}{\simeq} s_{\mu(\alpha_{2k-1}, \alpha_2)} \prod s_{\beta_i} \prod_{j \neq 1} s_{\alpha_j} = \left( \prod s_{\beta_i} \right) s_{\mu(\beta_{2k-2}, \beta_2)} \prod_{j \neq 1} s_{\alpha_j} = \\ &= \prod s_{\beta_i} \left( \prod_{j \neq 1} s_{\alpha_j} \right) s_{\mu(\alpha_{2k-2}, \alpha_3)} \stackrel{s_{\mu(\alpha_{2k-2}, \alpha_3)}}{\simeq} s_{\mu(\alpha_{2k-2}, \alpha_3)} \prod s_{\beta_i} \prod_{j \neq 1} s_{\alpha_j} = \left( \prod s_{\beta_i} \right) s_{\mu(\beta_{2k-3}, \beta_3)} \prod_{j \neq 1} s_{\alpha_j} = \\ &\dots \\ &= s_{\mu(\alpha_{k+1}, \alpha_k)} \prod s_{\beta_i} \prod_{j \neq 1} s_{\alpha_j}. \quad \square \end{aligned}$$

**Corollary 3.7.** *The conjugate class containing elements*

$$(s_{\mu(\alpha_{k+1}, \alpha_k)} \prod_{i=1}^{2k-1} s_{\beta_i}) (\prod_{i=2}^{2k-1} s_{\alpha_i}). \quad (3.24)$$

is associated with both  $D_l(b_{\frac{1}{2}l-1})$  and  $D_l(a_{\frac{1}{2}l-1})$ ,  $l = 4k - 2$ , Fig. 3.29.

For  $i \neq k$ , we need to check the orthogonality  $\mu(\alpha_{k+1}, \alpha_k) \perp \beta_i$ , and, for  $i = k$ , we have:

$$(\mu(\alpha_{k+1}, \alpha_k), \beta_k) = (\alpha_{k+1}, \beta_k) - (\alpha_k, \beta_k) = -\frac{1}{2} + \frac{1}{2} = 0.$$

For  $i \neq k, k+1$ , we have  $\mu(\alpha_{k+1}, \alpha_k) \perp \alpha_i$ , and, for  $i = k, k+1$ , we get:

$$\begin{aligned} (\mu(\alpha_{k+1}, \alpha_k), \alpha_k) &= (-\beta_{k-1}, \alpha_k) + (-\alpha_k, \alpha_k) = \frac{1}{2} - 1 = -\frac{1}{2}. \\ (\mu(\alpha_{k+1}, \alpha_k), \alpha_{k+1}) &= (\beta_{k+1}, \alpha_{k+1}) + (\alpha_{k+1}, \alpha_{k+1}) = 1 - \frac{1}{2} = \frac{1}{2}. \quad \square \end{aligned}$$

#### 4. The conjugacy class of the Carter diagram with a 4-cycle

**4.1. Uniqueness of the conjugacy class.** Conjugate elements in the Weyl group  $W$  are associated with the same Carter diagram  $\Gamma$ . Generally speaking, the converse is not true, the Carter diagram  $\Gamma$  does not determine a single conjugacy class in  $W$ , [Ca72, Lemma 27]. However, the converse statement takes place for the Carter diagrams containing at least one 4-cycle.

**Theorem 4.1.** *Let  $\Gamma$  be a Carter diagram containing at least one 4-cycle. Then  $\Gamma$  determines only one conjugacy class.*

The proof is divided into the following steps:

*Step 1.* For any two 4-cycles  $R_1$  and  $R_2$  associated with the same Weyl group, the equivalent diagonals in these cycles can be chosen, Lemma 4.3. The approach is a little different for diagrams  $E_n$  and  $D_n$ . The difference is due to unsuccessful location of the maximal root in the Dynkin diagram  $D_n$ , see Table A.6, Fig. A.44.

*Step 2.* The equivalence of two triples of roots in 4-cycles  $R_1$  and  $R_2$  can be extended to the equivalence of  $R_1$  and  $R_2$ , see Lemma 4.4. In Proposition 4.5, we show that any two 4-cycles  $R_1$  and  $R_2$  associated with the same Weyl group are equivalent. Lemma 4.4 and Proposition 4.5 are proved regardless of the choice of the Dynkin diagram. Hence, Theorem 4.1 is proven for  $D_4(a_1)$ ,  $E_6(a_2)$ ,  $E_7(a_4)$ ,  $E_8(a_6)$ .

*Step 3.* We show that the equivalence of two 4-cycles can be extended to the equivalence of 4-cycles extended by adding one edge (freely stemming from a vertex of every 4-cycle), see Lemma 4.6. This lemma is proved regardless of the choice of Dynkin diagram. Hence, Theorem 4.1 is proven for:  $D_5(a_1)$ ,  $E_6(a_1)$ ,  $E_7(a_2)$ ,  $E_7(a_3)$ ,  $E_8(a_3)$ ,  $E_8(a_5)$ ,  $E_8(a_7)$ , see Table 4.5.

*Step 4.* The equivalence of two diagrams containing 4-cycles and the tails of length  $n$  (freely stemming from a vertex of every 4-cycle) can be extended to the equivalence of 4-cycles extended by tails of length  $n+1$ , Lemma 4.7. This lemma is proved regardless of the choice of the Dynkin diagram. Hence, Theorem 4.1 is proven for  $E_7(a_1)$ ,  $E_8(a_1)$ ,  $E_8(a_2)$ ,  $E_8(a_4)$ .

For  $D_l(a_k)$ , where  $k > 2, l > 6$ , the equivalence follows from the fact for  $D_{l-1}(a_{k-1})$  by Lemma 4.7.

For  $D_l(a_2)$ , the equivalence follows from the fact for  $D_{l-1}(a_1)$  by Lemma 4.6.

For  $D_l(a_1)$ , where  $l > 6$ , the equivalence follows from the fact for  $D_{l-1}(a_1)$  by Lemma 4.7.

For  $D_5(a_1)$ , the equivalence follows from the fact for  $D_4(a_1)$  by Lemma 4.6.

**Remark 4.2.** In [St10, Proposition 3.6], we extended Theorem 4.1 to the class of Dynkin diagrams. Namely, for any Carter diagram  $\Gamma$  looking as either Dynkin diagrams  $D_n$  or  $E_n$ , the diagram  $\Gamma$  determines a single conjugacy class. The theorem does not hold for  $A_n$ , see [Ca72, p.31, Lemma 27] and [St10, Remark 3.7].

#### 4.2. Pair of orthogonal roots lying in 4-cycles.

**Lemma 4.3.** 1) For  $E_6, E_7, E_8$ , there is only one equivalence class of sets of 2 orthogonal roots under the Weyl group.

2) Each two 4-cycles in  $\Phi(D_n)$  contain diagonals equivalent each other under the action of  $W(D_n)$ .

*Proof.* 1) By Corollary A.5, for  $E_6, E_7, E_8$ , all sets of 2 orthogonal roots are equivalent under the corresponding Weyl group.

2) In the case of  $D_n$ , there is the following obstacle: the subset of roots orthogonal to the maximal root  $\alpha_{max}$  splits into the sum of two non-connected sets:

$$\alpha_{max} \perp \{\Phi(D_{n-2}) \oplus \Phi(A_1)\}, \quad (4.1)$$

see Fig. A.44, Table A.6. Let  $R_1 = \{\alpha_1, \alpha_2, \beta_1, \beta_2\}$  and  $R_2 = \{\delta_1, \delta_2, \varphi_1, \varphi_2\}$  be two 4-cycles from  $D_n$ . Since  $\Phi(A_1)$  consists of one root, at least one of the diagonals  $\{\alpha_1, \alpha_2\}$  or  $\{\beta_1, \beta_2\}$  belongs to  $\Phi(D_{n-2})$ . Thus, both  $R_1$  and  $R_2$  contain a diagonal from  $\Phi(D_{n-2})$  and these diagonals are equivalent under  $W(D_n)$ .  $\square$

**4.3. All 4-cycles are equivalent.** In the following lemma, we show that the map of triples of roots belonging to 4-cycles can be extended to the map of the 4-cycles themselves.

**Lemma 4.4** (extension of the map to the 4-cycle). *Let  $\mathcal{T}_1$  (resp.  $\mathcal{T}_2$ ) be the triple of roots in the 4-cycle  $\mathcal{C}_1$  (resp.  $\mathcal{C}_2$ ) associated with the same Carter diagram.*

*Let  $R_1 \supset \mathcal{T}_1$  and  $R_2 \supset \mathcal{T}_2$  be two subsets and  $U : R_1 \rightarrow R_2$  the map that sends the triple  $\mathcal{T}_1$  to the triple  $\mathcal{T}_2$  (as in Fig. 4.30:  $U\alpha_i = \delta_i, U\beta_j = \varphi_j$  for  $j \neq 3$ ). Then  $U$  can be extended to the map*

$$UC_1 = C_2 \text{ so that } U\beta_3 = \varphi_3.$$

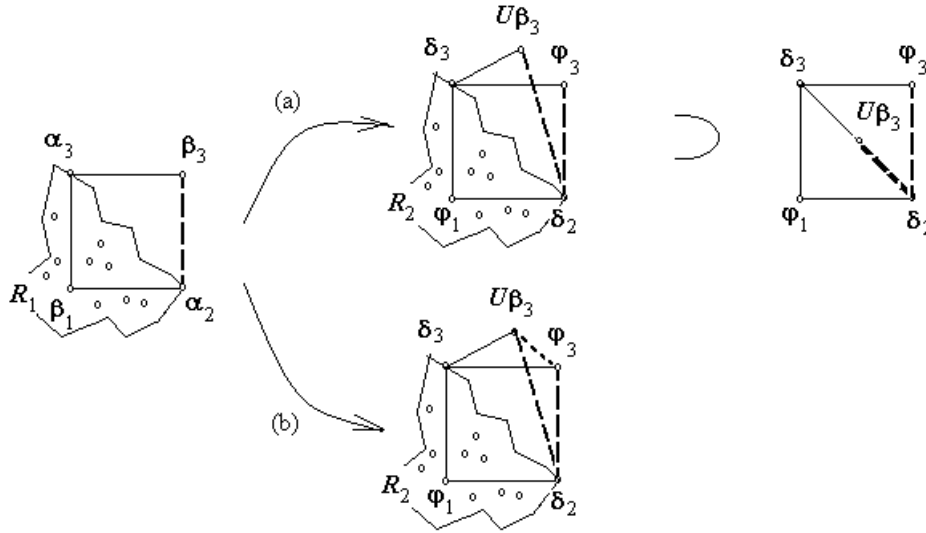


Figure 4.30. Extension of the map to the 4-cycle

*Proof.* Let  $\mathcal{C}_1 = \{\beta_1, \alpha_2, \beta_3, \alpha_3\}$  and  $\mathcal{C}_2 = \{\varphi_1, \delta_2, \varphi_3, \delta_3\}$  be two 4-cycles. Let  $U \in W$  be such that the map  $U : R_1 \rightarrow R_2$  acts on roots  $\beta_j \in R_1$  and  $\alpha_j \in R_1$ , where  $R_1, R_2$  are depicted as “clouds” in Fig. 4.30, as follows:

$$U\beta_i = \varphi_i \ (i \neq 3), \quad U\alpha_j = \delta_j,$$

We will show that there exists  $U' \in W$  such that

$$U' = U \text{ on } R_1 \text{ and } U'\beta_3 = \varphi_3. \quad (4.2)$$

Suppose  $\varphi_3 \neq U\beta_3$ . If  $U\beta_3$  is connected to both  $U\varphi_1$  and  $U\varphi_3$ , then the root  $U\beta_3$  is connected to all 4 vertices of the 4-cycle, contradicting Corollary 2.4. If  $U\beta_3$  is connected to  $U\varphi_1$  we have the same case as (b) in Fig. 4.30. For the case (a), the diagram contains two cycles with the intersection  $\{\delta_2, U\beta_3, \delta_3\}$  of the length more than 1 edge, contradicting Corollary 2.4, heading 1). So, only case (b) is possible. We have two root sets:

$$\begin{aligned} &\{\delta_2, \delta_3, \varphi_1, \varphi_3\}, \\ &\{\delta_2, \delta_3, \varphi_1, U\beta_3\}. \end{aligned} \quad (4.3)$$

In (4.3), the bottom set can be obtained from the top one by the transformation  $T = s_{U\beta_3}s_{\varphi_3}s_{U\beta_3}$ :

$$\begin{aligned} s_{U\beta_3}s_{\varphi_3}s_{U\beta_3}(\varphi_3) &= U\beta_3, \\ s_{U\beta_3}s_{\varphi_3}s_{U\beta_3}(\delta_3) &= s_{U\beta_3}s_{\varphi_3}(\delta_3 + U\beta_3) = s_{U\beta_3}(\delta_3 + \varphi_3 + U\beta_3 - \varphi_3) = \\ &= s_{U\beta_3}(\delta_3 + U\beta_3) = \delta_3, \\ s_{U\beta_3}s_{\varphi_3}s_{U\beta_3}(\delta_2) &= s_{U\beta_3}s_{\varphi_3}(\delta_2 - U\beta_3) = s_{U\beta_3}(\delta_2 - \varphi_3 - U\beta_3 + \varphi_3) = \\ &= s_{U\beta_3}(\delta_2 - U\beta_3) = \delta_2. \end{aligned} \quad (4.4)$$

Then  $U' = T^{-1}U$ . □

By Lemma 4.4 every diagonal of any 4-cycle  $R_1$  can be sent to one of diagonals of the other 4-cycle  $R_2$ . In the following proposition, we show that there can be found an element  $U \in W$  mapping the second diagonal of  $R_1$  to the second diagonal of  $R_2$ .

**Proposition 4.5** (equivalence of 4-cycles). *Let  $R_1 = \{\beta_1, \alpha_2, \alpha_3, \beta_3\}$  and  $R_2 = \{\varphi_1, \delta_2, \delta_3, \varphi_3\}$  be two squares and  $U : R_1 \rightarrow R_2$  an element of the Weyl group such that*

$$U\alpha_2 = \delta_2, \quad U\alpha_3 = \delta_3 \text{ (equivalence of diagonals of } R_1 \text{ and } R_2).$$

*Then there exists  $U' \in W$ , such that*

$$U'\alpha_2 = \delta_2, \quad U'\alpha_3 = \delta_3, \quad U'\beta_1 = \varphi_1, \quad U'\beta_3 = \varphi_3.$$

*Proof.* The possible cases (a), (b), (c) of the map  $U : R_1 \rightarrow R_2$  are given in Fig. 4.31. The case

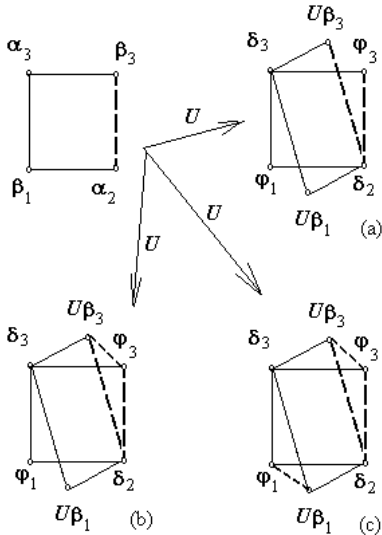


Figure 4.31.

$U\beta_1 = \varphi_1$  (resp.  $U\beta_3 = \varphi_3$ ) is considered in Lemma 4.4, (b). Suppose  $U\beta_1 \neq \varphi_1$  and  $U\beta_3 \neq \varphi_3$ . In the case (a) in Fig. 4.31, we remove the root  $\delta_2$ ; the remaining diagram  $\{\delta_3, \varphi_1, U\beta_1, U\beta_3, \varphi_3\}$  is  $\tilde{D}_4$ , contradicting Proposition A.2. In the case (b) (resp. the opposite one, where  $\varphi_1$  and  $U\beta_1$  are connected, and  $\varphi_3$  and  $U\beta_3$  are non-connected), we remove the root  $U\beta_3$ , then the remaining diagram can not occur by Corollary 2.4, heading 1). The case where  $U\beta_1$  (resp.  $U\beta_3$ ) is connected with both  $\varphi_1$  and  $\varphi_3$  can not occur by Corollary 2.4, heading 2). Consider case (c). As above, in (4.4), we correct  $U$  by the transformation  $T = s_{U\beta_3}s_{\varphi_3}s_{U\beta_3}$ , i.e.,  $U' = T^{-1}U$  preserves  $\delta_2, \delta_3, \varphi_1, U\beta_1$  and sends  $\varphi_3$  to the root  $U\beta_3$ . Similarly, we correct  $U'$  by the transformation  $P = s_{U\beta_1}s_{\varphi_1}s_{U\beta_1}$ , i.e.,  $U'' = P^{-1}U'$  preserves  $\delta_2, \delta_3, \varphi_3 = U\beta_3$  and sends  $\varphi_1$  to the root  $U\beta_1$ , see Lemma 4.4, (b). □

#### 4.4. The vertex with the branching degree $\geq 3$ .

**Lemma 4.6** (branch vertex, degree  $\geq 3$ ). *Let  $\mathcal{T}_1$ , (resp.  $\mathcal{T}_2$ ) be the triple of roots in the root subset  $\mathcal{D}_1$  (resp.  $\mathcal{D}_2$ ) of type  $D_4$  associated with the same Carter diagram;  $\mathcal{T}_1$  (resp.  $\mathcal{T}_2$ ) contains the branch point of  $\mathcal{D}_1$  (resp.  $\mathcal{D}_2$ ).*

Let  $R_1 \supset \mathcal{T}_1$ ,  $R_2 \supset \mathcal{T}_2$  be two subsets and  $U : R_1 \longrightarrow R_2$  be the map such that the triple  $\mathcal{T}_1$  is mapped to the triple  $\mathcal{T}_2$  (as in Fig. 4.32:  $U\alpha_i = \delta_i$ ,  $U\beta_j = \varphi_j$  for  $j \neq 2$ ). Then  $U$  can be extended to the map

$$U\mathcal{D}_1 = \mathcal{D}_2 \text{ so that } U\beta_2 = \varphi_2.$$

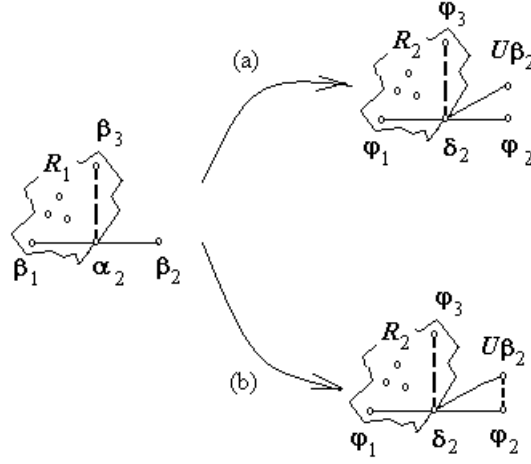


Figure 4.32. The branch point with branching degree  $\geq 3$

*Proof.* Let  $\mathcal{D}_1 = \{\alpha_2, \beta_1, \beta_2, \beta_3\}$  and  $\mathcal{D}_2 = \{\delta_2, \varphi_1, \varphi_2, \varphi_3\}$ . Let  $U \in W$  be such that the map  $U : R_1 \longrightarrow R_2$  acts on all roots  $\beta_i \in R_1$  and  $\alpha_j \in R_1$ , where  $R_1, R_2$  are depicted as “clouds” in Fig. 4.32, as follows:

$$U\beta_i = \varphi_i \ (i \neq 2), \quad U\alpha_j = \delta_j,$$

There exists  $U' \in W$  such that

$$U' = U \text{ on } R_1 \text{ and } U'\beta_2 = \varphi_2. \quad (4.5)$$

Suppose  $\varphi_2 \neq U\beta_2$ . Since  $U$  preserves connections, then  $U\beta_2$  is connected with  $\delta_2$ , Fig. 4.32,(a). Perhaps  $U\beta_2$  is also connected with  $\varphi_2$ , Fig. 4.32,(b). Case (a) in Fig. 4.32 can not occur, otherwise we obtain the root subset  $\{\varphi_1, \varphi_2, \varphi_3, \delta_2, U\beta_2\}$  corresponding to the extended Dynkin diagram  $\tilde{D}_4$ . The case (b) in Fig. 4.32 is possible, and we have two root subsets:

$$\begin{aligned} &\{\delta_2, \varphi_1, \varphi_2, \varphi_3\}, \\ &\{\delta_2, \varphi_1, U\beta_2, \varphi_3\}. \end{aligned} \quad (4.6)$$

In (4.6) the bottom set can be obtained from the top one by the transformation  $T = s_{U\beta_2} s_{\varphi_2} s_{U\beta_2}$ :

$$\begin{aligned} s_{U\beta_2} s_{\varphi_2} s_{U\beta_2}(\varphi_2) &= U\beta_2, \\ s_{U\beta_2} s_{\varphi_2} s_{U\beta_2}(\delta_2) &= s_{U\beta_2} s_{\varphi_2}(\delta_2 + U\beta_2) = s_{U\beta_2}(\delta_2 + \varphi_2 + U\beta_2 - \varphi_2) = \\ &= s_{U\beta_2}(\delta_2 + U\beta_2) = \delta_2. \end{aligned}$$

All other roots are not changed under  $T$ . We have  $U' = T^{-1}U$ . □

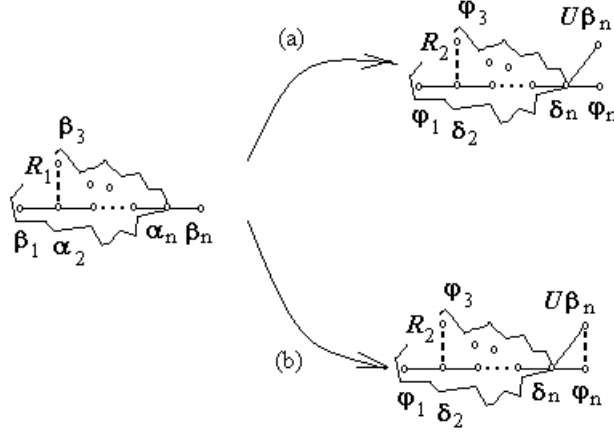
#### 4.5. The tail stemming from 4-cycle.

**Lemma 4.7** (tails of length  $> 1$ ). *Let  $\mathcal{T}_1$ , (resp.  $\mathcal{T}_2$ ) be the root subset of type  $D_{2n-2}$  in the root subset  $\mathcal{D}_1$  (resp.  $\mathcal{D}_2$ ) of type  $D_{2n-1}$ , such that  $\mathcal{D}_1$  and  $\mathcal{D}_2$  are associated with the same Carter diagram.*

*Let  $R_1 \supset \mathcal{T}_1$  and  $R_2 \supset \mathcal{T}_2$  be two subsets and  $U : R_1 \longrightarrow R_2$  the map such that the root subset  $\mathcal{T}_1$  is mapped to the root subset  $\mathcal{T}_2$  (as in Fig. 4.33:  $U\alpha_i = \delta_i$ ,  $U\beta_j = \varphi_j$  for  $j \neq n$ ).*

*Then  $U$  can be extended to the map*

$$U\mathcal{D}_1 = \mathcal{D}_2 \text{ so that } U\beta_n = \varphi_n.$$

Figure 4.33. Transformation  $U : R_1 \longrightarrow R_2$ ;  $\beta_2$  connected to  $R_1$  in  $\alpha_2$ 

*Proof.* Let  $\mathcal{D}_1 = \{\beta_1, \dots, \beta_n, \alpha_2, \dots, \alpha_n\}$  and  $\mathcal{D}_2 = \{\varphi_1, \dots, \varphi_n, \delta_2, \dots, \delta_n\}$  be the root subsets associated with the same Carter diagram. Let  $U \in W$  such that the map  $U : R_1 \longrightarrow R_2$  acts on all roots  $\beta_i \in R_1$  and  $\alpha_j \in R_1$ , where  $R_1, R_2$  are depicted as “clouds” in Fig. 4.33), as follows:

$$U\beta_i = \varphi_i \ (i \neq n), \quad U\alpha_j = \delta_j.$$

We will show that there exists  $U' \in W$  such that

$$U' = U \text{ on } R_1 \text{ and } U'\beta_n = \varphi_n. \quad (4.7)$$

Suppose  $\varphi_n \neq U\beta_n$ . Since  $U$  preserves connections, then  $U\beta_n$  is connected with  $\delta_n$ , Fig. 4.33,(a), and, as above, perhaps is connected with  $\varphi_n$ , Fig. 4.33,(b). Case (a) in Fig. 4.33 can not occur, otherwise the diagram in the right side contains the extended Dynkin diagram  $\tilde{D}_{2n-1}$ , ( $n \geq 2$ ). The case (b) in Fig. 4.33,(b) is possible, and we have two root subsets:

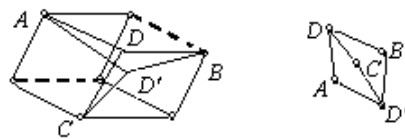
$$\begin{aligned} &\{\varphi_1, \delta_2, \dots, \delta_n, \varphi_n, \varphi_3\}, \\ &\{\varphi_1, \delta_2, \dots, \delta_n, U\beta_n, \varphi_3\}. \end{aligned} \quad (4.8)$$

The bottom set in (4.8) can be obtained from the top one by the transformation  $T = s_{U\beta_n} s_{\varphi_n} s_{U\beta_n}$ .

$$\begin{aligned} s_{U\beta_n} s_{\varphi_n} s_{U\beta_n}(\varphi_n) &= U\beta_n, \\ s_{U\beta_n} s_{\varphi_n} s_{U\beta_n}(\delta_n) &= s_{U\beta_n} s_{\varphi_n}(\delta_n + U\beta_n) = s_{U\beta_n}(\delta_n + \varphi_n + U\beta_n - \varphi_n) = \\ &= s_{U\beta_n}(\delta_n + U\beta_n) = \delta_n. \end{aligned}$$

All other roots are not changed under  $T$ , and  $U' = T^{-1}U$ .  $\square$

**4.6. Four patterns of root subsets.** Now, by means of steps from Section 4.1, we can prove that there is only one conjugacy class associated with every connected Carter diagram. This fact is proved by means of Proposition 4.5 (4-cycles equivalence), Lemma 4.4 (extension to a 4-cycle), Lemma 4.6 (branch vertex, degree  $\geq 3$ ), and Lemma 4.7 (tails of length  $> 1$ ), see Table 4.5.

Figure 4.34. The case  $E_8(a_8)$

The last case is the diagram  $E_8(a_8)$ . This diagram is constructed from  $E_7(a_4)$  by attaching one vertex  $D$ , Fig. 4.34. If there are two different points  $D$  and  $D'$  as in Fig. 4.34, we get two cycles intersecting on the border  $DCD'$  of length  $> 1$  contradicting Proposition 2.3.

## APPENDIX A. Some properties of the Carter and Dynkin diagrams

**A.1. The ratio of lengths of roots.** Let  $\Gamma$  be a Dynkin diagram, and  $\sqrt{t}$  be the ratio of lengths of long and short roots. The inner product between two long roots is

$$(\alpha, \beta) = \sqrt{t} \cdot \sqrt{t} \cdot \cos(\widehat{\alpha, \beta}) = \sqrt{t} \cdot \sqrt{t} \cdot (\pm \frac{1}{2}) = \pm \frac{t}{2}.$$

According to Remark 1.6, we put  $(\alpha, \beta) = -\frac{t}{2}$ . The inner product between two short roots is

$$(\alpha, \beta) = \cos(\widehat{\alpha, \beta}) = \pm \frac{1}{2}.$$

Again, according to Remark 1.6, we put  $(\alpha, \beta) = -\frac{1}{2}$ . The inner product  $(\alpha, \beta)$  between roots of different lengths is

$$(\alpha, \beta) = 1 \cdot \sqrt{t} \cdot \cos(\widehat{\alpha, \beta}) = 1 \cdot \sqrt{t} \cdot (\pm \frac{\sqrt{t}}{2}) = \pm \frac{t}{2}.$$

As above, we choose the obtuse angle and we put  $(\alpha, \beta) = -\frac{t}{2}$ .

## A.2. Cycles in simply-laced case.

### A.2.1. The Carter and connection diagrams for trees.

**Lemma A.1.** *There are no a root subset (in the root system associated with a Dynkin diagram) forming a simply-laced cycle containing only solid edges. Any cycle in the Carter diagram or in the connection diagram contains at least one solid edge and at least one dotted edge.*

*Proof.* Suppose the subset  $S = \{\alpha_1, \dots, \alpha_n\} \subset \Phi$  forms a cycle containing only solid edges. Consider the vector

$$v = \sum_{i=1}^n \alpha_i.$$

The value of quadratic Tits form  $\mathcal{B}$  (see [St08]) on  $v$  is

$$\mathcal{B}(v) = \sum_{i \in \Gamma_0} 1 - \sum_{i \in \Gamma_1} 1 = n - n = 0,$$

where  $\Gamma_0$  (resp.  $\Gamma_1$ ) is the set of all vertices (resp. edges) of the diagram associated with  $S$ . Therefore,  $v = 0$  and elements of the root subset  $S$  are linearly dependent.  $\square$

The following proposition is true only for trees.

**Proposition A.2** (Lemma 8, [Ca72]). *Let  $S = \{\alpha_1, \dots, \alpha_n\}$  be the root subset of linearly independent (not necessarily simple) roots from the root system  $\Phi$  associated with a certain Dynkin diagram  $\Gamma$ , and let  $\Gamma_S$  be the Carter diagram or the connection diagram associated with  $S$ . If  $\Gamma_S$  is a tree, then  $\Gamma_S$  is a Dynkin diagram.*

Name	The Carter diagram	Follows from (pattern)	Basic diagram
$D_4(a_1)$		<i>Proposition 4.5</i> (4-cycles equivalence)	-
$D_5(a_1)$		<i>Lemma 4.6</i> (branch vertex, degree $\geq 3$ )	$D_4(a_1)$
$E_6(a_1)$		<i>Lemma 4.6</i> (branch vertex, degree $\geq 3$ )	$D_5(a_1)$
$E_6(a_2)$		<i>Lemma 4.4</i> (extension to a 4-cycle)	$D_5(a_1)$
$E_7(a_1)$		<i>Lemma 4.7</i> (tails of length $> 1$ )	$E_6(a_1)$
$E_7(a_2)$		<i>Lemma 4.6</i> (branch vertex, degree $\geq 3$ )	$E_6(a_1)$
$E_7(a_3)$		<i>Lemma 4.6</i> (branch vertex, degree $\geq 3$ )	$E_6(a_2)$
$E_7(a_4)$		<i>Lemma 4.4</i> (extension to a 4-cycle)	$E_6(a_2)$
$E_8(a_1)$		<i>Lemma 4.7</i> (tails of length $> 1$ )	$E_7(a_1)$
$E_8(a_2)$		<i>Lemma 4.7</i> (tails of length $> 1$ )	$E_7(a_1)$
$E_8(a_3)$		<i>Lemma 4.6</i> (branch vertex, degree $\geq 3$ )	$E_7(a_2)$
$E_8(a_4)$		<i>Lemma 4.7</i> (tails of length $> 1$ )	$E_7(a_3)$
$E_8(a_5)$		<i>Lemma 4.6</i> (branch vertex, degree $\geq 3$ )	$E_7(a_3)$
$E_8(a_6)$		<i>Lemma 4.4</i> (extension to a 4-cycle)	$E_7(a_3)$
$E_8(a_7)$		<i>Lemma 4.6</i> (branch vertex, degree $\geq 3$ )	$E_7(a_4)$
$E_8(a_8)$		<i>Proposition 2.3</i> (intersection of two cycles)	$E_7(a_4)$
$D_l(a_k)$		<i>Lemma 4.6</i> (branch vertex, degree $\geq 3$ ) <i>Lemma 4.7</i> (tails of length $> 1$ )	$D_l(a_{k-1})$ for $k > 1$ , $D_{l-1}(a_1)$ for $k = 1, l > 5$

Table 4.5. Uniqueness of the conjugacy class characterized by the simply-laced Carter diagram with 4-cycles



*Proof.* If  $\Gamma_S$  is not a Dynkin diagram, then  $\Gamma_S$  contains an extended Dynkin diagram  $\tilde{\Gamma}$  as a subdiagram. Since  $\Gamma_S$  is a tree, we can turn all dotted edges to solid ones<sup>1</sup>, see Remark 1.6. Further, we consider the vector

$$v = \sum_{i \in \tilde{\Gamma}_0} t_i \alpha_i, \quad (\text{A.1})$$

where  $\tilde{\Gamma}_0$  is the set of all vertices of  $\tilde{\Gamma}$ , and  $t_i (i \in \tilde{\Gamma}_0)$  are the coefficients of the nil-root, see [Kac80]. Let the remaining coefficients corresponding to  $\Gamma_S \setminus \tilde{\Gamma}$  be equal to 0. Let  $\mathcal{B}$  be the positive definite quadratic Tits form [St08] associated with the diagram  $\Gamma$ , and  $(\ , \ )$  the symmetric bilinear form associated with  $\mathcal{B}$ . Let  $\{\delta_i\}$  be the set of simple roots associated with vertices  $\tilde{\Gamma}_0$ . For all  $i, j \in \tilde{\Gamma}_0$ , we have  $(\alpha_i, \alpha_j) = (\delta_i, \delta_j)$ , since this value is described by edges of  $\tilde{\Gamma}$ . Therefore

$$\mathcal{B}(v) = \sum_{i, j \in \tilde{\Gamma}_0} t_i t_j (\alpha_i, \alpha_j) = \sum_{i, j \in \tilde{\Gamma}_0} t_i t_j (\delta_i, \delta_j) = \mathcal{B}\left(\sum_{i \in \tilde{\Gamma}_0} t_i \delta_i\right) = 0.$$

Since  $\mathcal{B}$  is the positive definite form, we have  $v = 0$ , i.e., vectors  $\alpha_i$  are linearly dependent that contradicts the definition of the set  $S$ .  $\square$

**Example A.3** (multiply-laced cases). On Fig. A.35, Fig. A.36, Fig. A.37 and Fig. A.38, we put the coefficients of the linear dependence be as in the proof of Proposition A.2. In all cases below,  $\sqrt{t}$  is the ratio of lengths of long and short roots; the inner product between long roots or between long and short roots is  $-\frac{t}{2}$ , the inner product between two short roots is  $-\frac{1}{2}$ , see Section A.1. The labels in vertices are coordinates of nil-root of the corresponding extended Dynkin diagrams, [Kac80].

$$\tilde{F}_{41} \quad \begin{array}{cccccc} \alpha & \text{---} & \beta & \text{---} & \gamma & \text{---} & \delta & \text{---} & \varphi \\ 1 & & 2 & & 3 & & 2 & & 1 \end{array}$$

Case  $\tilde{F}_{41}$ . Let  $v = \alpha + 2\beta + 3\gamma + 2\delta + \varphi$ . Then

$$\|v\| = 1 + 4 + 9 + 4t + t - 1 \cdot 2 - 2 \cdot 3 - 3 \cdot 2t - 2 \cdot t = 6 - 3t = 0 \text{ since } t = 2.$$

$$\tilde{F}_{42} \quad \begin{array}{cccccc} \alpha & \text{---} & \beta & \text{---} & \gamma & \text{---} & \delta & \text{---} & \varphi \\ 1 & & 2 & & 3 & & 4 & & 2 \end{array}$$

Case  $\tilde{F}_{42}$ . Here,  $v = \alpha + 2\beta + 3\gamma + 4\delta + 2\varphi$ , and

$$\|v\| = (1 + 4 + 9)t + 16 + 4 - 1 \cdot 2t - 2 \cdot 3t - 3 \cdot 4t - 4 \cdot 2 = 12 - 6t = 0 \text{ since } t = 2.$$

Figure A.35.

Case  $\tilde{C}_2$ . Consider  $v = \alpha + t\beta + \gamma$ , where  $t = 2$ . Then

$$\|v\| = t + t^2 + t - t \cdot t - t \cdot t = 2t - t^2 = 0.$$

$$\tilde{C}_2 \quad \begin{array}{ccccc} \alpha & \text{---} & \beta & \text{---} & \gamma \\ 1 & & 2 & & 1 \end{array}$$

Case  $\tilde{B}_2$ . Set  $v = \alpha + \beta + \gamma$ . Then

$$\|v\| = 1 + 1 + t - t - t = 2 - t = 0.$$

$$\tilde{B}_2 \quad \begin{array}{ccccc} \alpha & \text{---} & \beta & \text{---} & \gamma \\ 1 & & 1 & & 1 \end{array}$$

Figure A.36.

$$\tilde{C}_3 \quad \begin{array}{ccccccc} \alpha & \text{---} & \beta & \text{---} & \gamma & \text{---} & \delta \\ 1 & & 2 & & 2 & & 1 \end{array}$$

Case  $\tilde{C}_3$ . We put  $v = \alpha + t\beta + t\gamma + \delta$ , and

$$\|v\| = t + t + t^2 + t^2 - t^2 - t^2 - t^2 = 2t - t^2 = 0.$$

$$\tilde{B}_3 \quad \begin{array}{ccccccc} \alpha & \text{---} & \beta & \text{---} & \gamma & \text{---} & \delta \\ 1 & & 1 & & 1 & & 1 \end{array}$$

Case  $\tilde{B}_3$ . Consider  $v = \alpha + \beta + \gamma + \delta$ . Then

$$\|v\| = 1 + 1 + t + t - t - t - t = 2 - t.$$

Figure A.37.

<sup>1</sup>This fact is not true for cycles, since by Lemma A.1 we can not eliminate all dotted edges.

For  $\tilde{C}_n$ , where  $n \geq 4$ , we put  $v = \alpha_1 + t\alpha_2 + \cdots + t\alpha_n + \alpha_{n+1}$ . Any new short edge adds  $t^2 - t^2$ , i.e.,  $\|v\| = 0$ . For  $\tilde{B}_n$ , where  $n \geq 4$ , we put  $v = \alpha_1 + \alpha_2 + \cdots + \alpha_n + \alpha_{n+1}$ . Any new long edge adds  $t - t$ , i.e.,  $\|v\| = 0$ .

Case  $\tilde{G}_{21}$ . Consider  $v = \alpha + 2\beta + \gamma$ . Here,  $t = 3$ . Then

$$\|v\| = 1 + 4 + t - 1 \cdot 2 - 2 \cdot t = 3 - t = 0.$$

$$\tilde{G}_{21} \quad \alpha \xrightarrow{1} \beta \xRightarrow{2} \gamma$$

Case  $\tilde{G}_{22}$ . Consider  $v = \alpha + 2\beta + 3\gamma$ . Again,  $t = 3$ . Then

$$\|v\| = t + 4 \cdot t + 9 - 2 \cdot t - 2 \cdot 3 \cdot t = 9 - 3t = 0.$$

$$\tilde{G}_{22} \quad \alpha \xrightarrow{1} \beta \xRightarrow{2} \gamma$$

Figure A.38.

□

A.2.2. *There are no cycles for the diagram  $A_n$ .* Remember that any root in  $A_n$  is of the form  $\pm(e_i - e_j)$ ,  $1 \leq i < j \leq n + 1$ . Then, up to an  $s_\alpha$ -reflection  $\alpha \rightarrow -\alpha$ , see Section 1.4.1, a cycle of roots is of one of the followings forms:

$$\begin{aligned} &\{e_{i_1} - e_{i_2}, e_{i_2} - e_{i_3}, \dots, e_{i_{k-1}} - e_{i_k}, e_{i_k} - e_{i_1}\}, \\ &\{e_{i_1} - e_{i_2}, e_{i_2} - e_{i_3}, \dots, e_{i_{k-1}} - e_{i_k}, -(e_{i_k} - e_{i_1})\}. \end{aligned}$$

In the first case, the sum of all these roots is 0, and roots are linearly dependent. In the second case, the sum of the  $k - 1$  first roots is equal to the last one, and roots are also linearly dependent. Thus, for  $A_n$ , there are no cycles of linearly independent roots.

### A.3. Cycles in the multiply-laced case.

A.3.1. *4-cycle with all obtuse angles can not be.* The root system  $R$  containing the 4-cycle with all obtuse angles can not occur. Suppose this case is possible, so the root quadruple  $\{\alpha, \beta, \gamma, \delta\}$  yields pairs with the following values of the Tits form:

$$(\alpha, \beta) = -1, \quad (\beta, \gamma) = -\frac{1}{2}, \quad (\gamma, \delta) = -1, \quad (\delta, \alpha) = -1,$$

see Fig. A.39.

$$\begin{aligned} s_\alpha &= \begin{pmatrix} -1 & 1 & 0 & 1 \\ 0 & 1 & 0 & 0 \\ 0 & 0 & 1 & 0 \\ 0 & 0 & 0 & 1 \end{pmatrix}, s_\beta = \begin{pmatrix} 1 & 0 & 0 & 0 \\ 2 & -1 & 1 & 0 \\ 0 & 0 & 1 & 0 \\ 0 & 0 & 0 & 1 \end{pmatrix}, \\ s_\gamma &= \begin{pmatrix} 1 & 0 & 0 & 0 \\ 0 & 1 & 0 & 0 \\ 0 & 1 & -1 & 2 \\ 0 & 0 & 0 & 1 \end{pmatrix}, s_\delta = \begin{pmatrix} 1 & 0 & 0 & 0 \\ 0 & 1 & 0 & 0 \\ 0 & 0 & 1 & 0 \\ 1 & 0 & 1 & -1 \end{pmatrix}. \end{aligned}$$

Then the primitive (semi-Coxeter) element  $\mathbf{C} = s_\alpha s_\beta s_\gamma s_\delta$  in the Weyl group generated by the quadruple  $\{s_\alpha, s_\beta, s_\gamma, s_\delta\}$  and its characteristic polynomial are as follows:

$$\mathbf{C} = s_\alpha s_\beta s_\gamma s_\delta = \begin{pmatrix} 4 & 0 & 2 & -3 \\ 4 & 0 & 1 & -2 \\ 2 & 1 & 1 & -2 \\ 1 & 0 & 1 & -1 \end{pmatrix}, \quad \chi(\mathbf{C}) = x^4 - 4x^3 - x^2 - 4x + 1.$$

Since  $\chi(\mathbf{C})$  has a maximal root  $\lambda \approx 4.419 > 1$  then the primitive element  $\mathbf{C}$  is of the infinite order that can not be.

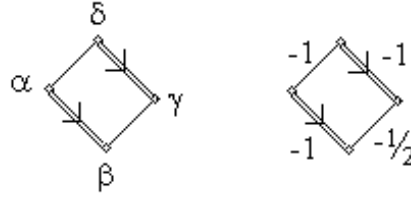
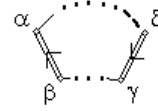


Figure A.39.

**A.3.2. More impossible cases of multiply-laced cycles.** In that follows, we consider several patterns (of multiply-laced diagrams) that are not a part of any Carter diagram. First of all, the arrows on the double edges connecting roots of different lengths should be directed face to face, otherwise we have the 3 different lengths of roots, as depicted in Fig. A.40:



$$\|\delta\| > \|\gamma\| = \|\beta\| > \|\alpha\|.$$

Figure A.40.



Figure A.41.

Further, two double edges connecting roots of different lengths cannot be adjacent, as depicted in Fig. A.41. Otherwise, the root subset contains extended Dynkin diagram  $\tilde{B}_2$  or  $\tilde{C}_2$  that can not occur.

For cycles of length 5 or more, the diagram contains the extended Dynkin diagram of type  $\tilde{B}_n$  or  $\tilde{C}_n$  that can not be. If the acute angle (resp. the dotted edge) lies on the part corresponding  $\tilde{B}_n$  (or  $\tilde{C}_n$ ) this obstacle can be easily eliminated by changing certain roots to their opposites; the procedure of eliminating the acute angle may be applied to any tree regardless whether it contains roots of different lengths or not.

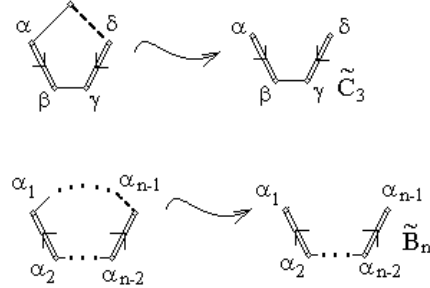


Figure A.42.

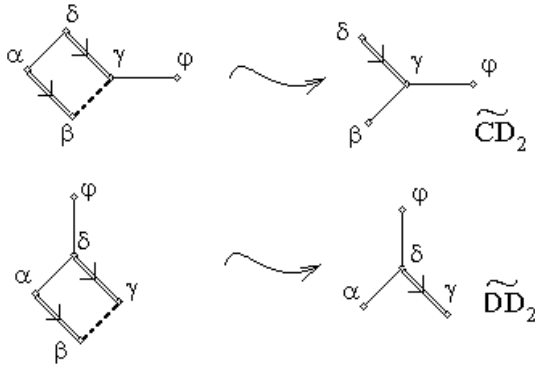
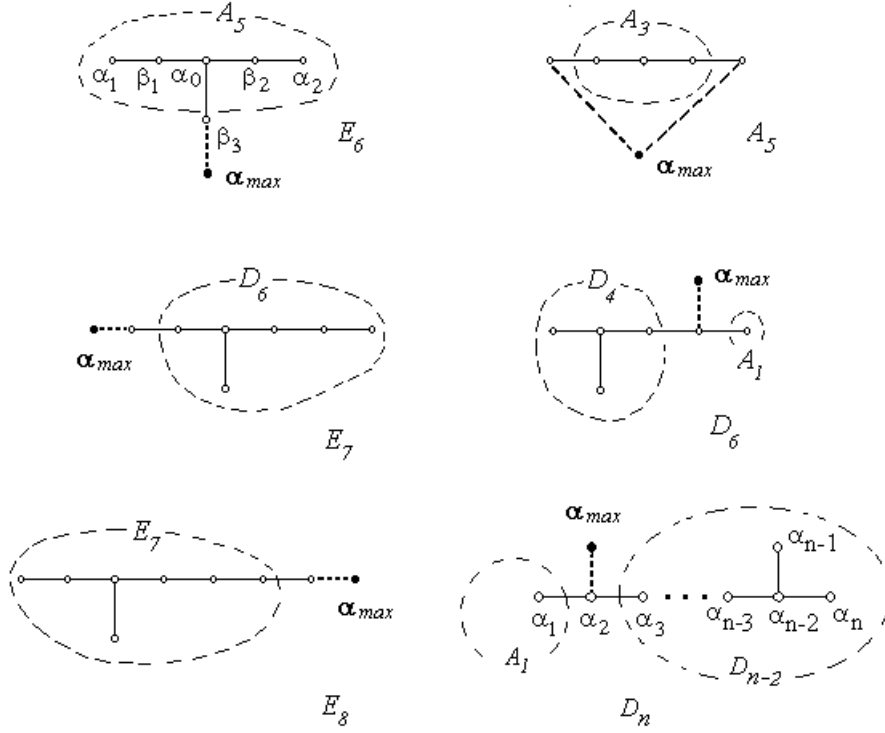


Figure A.43.

There are no cycles of length 4 with an additional fifth edge, since any such subset contains extended Dynkin diagram  $\tilde{CD}_2$  or  $\tilde{DD}_2$  that can not be, see Fig. A.43. One should note that any cycle in the Carter diagram contains an even number of vertices, so the connection like  $\{\varphi, \alpha\}$  or  $\{\varphi, \beta\}$  forming a triangle can not occur.

Figure A.44. Subsets of orthogonal roots in  $\Phi(D_n)$ ,  $\Phi(E_n)$ 

	The root system $D$	The maximal root $\alpha_{max}$ in the root system $\Phi(D)$	The root $\eta \in \Phi(D)$ , $\eta \perp \alpha_{max}$ if and only if $\eta \in \Phi(D')$ , $D' \subset D$
1	$E_6$	$\alpha_{max} \in \Phi(E_6)$	$\eta \in \Phi(A_5)$
2	$A_5$	$\alpha_{max} \in \Phi(A_5)$	$\eta \in \Phi(A_3)$
3	$E_7$	$\alpha_{max} \in \Phi(E_7)$	$\eta \in \Phi(D_6)$
4	$D_6$	$\alpha_{max} \in \Phi(D_6)$	$\eta \in \Phi(D_4) \oplus \Phi(A_1)$
5	$E_8$	$\alpha_{max} \in \Phi(E_8)$	$\eta \in \Phi(E_7)$
6	$D_n$	$\alpha_{max} \in \Phi(D_n)$	$\eta \in \Phi(D_{n-2}) \oplus \Phi(A_1)$

Table A.6. Roots  $\eta \in \Phi(D)$  such that  $\eta \perp \alpha_{max}$ 

**A.4. Subsets of mutually orthogonal roots.** In the following lemma, we show that for  $E_6$  (resp.  $E_8$ ) any two subsets of 3 orthogonal roots are equivalent under  $W = W(E_6)$  (resp.  $W = W(E_8)$ ). This statement is not correct for  $E_7$ , because of the different behavior of  $E_7$ : an “unlucky” location of the maximal root with respect to the Dynkin diagram, Fig. A.44. Remember that the location of the maximal root is the same as the additional vertex in the extended Dynkin diagram, [Bo].

**Lemma A.4.** *Let the root  $\alpha_{max}$  be the maximal root of the root system  $\Phi(D)$ , where  $D$  is given by Table A.6, column 2. The maximal root  $\alpha_{max} \in \Phi(D)$  is orthogonal to the root  $\eta \in \Phi(D)$  if and only if  $\eta \in D'$ , where  $D' \subset D$  are given by Table A.6, column 4.*

*Proof.* 1) Consider line 1 of Table A.6. We need to prove that the maximal root  $\alpha_{max}$  in  $\Phi(E_6)$  is orthogonal to the root  $\eta \in \Phi(E_6)$  if and only if  $\eta \in \Phi(A_5) = \{\alpha_0, \alpha_1, \alpha_2, \beta_1, \beta_2\}$ , see Fig. A.44. The maximal root  $\alpha_{max}$  in  $\Phi(E_6)$  is as follows:

$$\alpha_{max} = \alpha_1 + 2\beta_1 + 3\alpha_0 + 2\beta_2 + \alpha_2 + 2\beta_3, \text{ and}$$

$$\alpha_{max} \perp \alpha_i, \text{ for } i = 0, 1, 2; \quad \alpha \perp \beta_1, \beta_2, \text{ and } \alpha \not\perp \beta_3.$$

Therefore,  $\alpha_{max}$  is orthogonal to  $\Phi(A_5)$  spanned by  $\{\alpha_0, \alpha_1, \alpha_2, \beta_1, \beta_2\}$ . Any root  $\eta$  from  $\Phi(E_6)$  has the form  $\eta = k_1 z + k_2 \beta_3$ , where  $z \in \Phi(A_5)$ . Since  $\alpha_{max} \perp z$  and  $\alpha_{max} \not\perp \beta_3$ , then  $\alpha_{max} \perp \eta$  means that  $k_2 = 0$ , and  $\eta \in \Phi(A_5)$ . If  $\alpha_{max} \in \Phi(A_5)$  the similar arguments show that  $\eta \in \Phi(A_5)$ ,  $\eta \perp \alpha_{max}$  if and only if  $\eta \in A_3$ , see Fig. A.44. The remaining cases 2) - 6) from Table A.6 are similarly considered.  $\square$

**Corollary A.5.** 1) Any two sets of 2 orthogonal roots in  $\Phi(D)$ , where  $D = E_6, E_7, E_8$ , are equivalent under  $W(D)$ .

2) There are two sets of 2 orthogonal roots in  $\Phi(D_n)$  which are not equivalent under  $W(D_n)$ , (see Fig. A.44 and Table A.6).  $\square$

**Corollary A.6.** ([Ca72, Lemma 11,(i), Lemma 27]) 1) Any two sets of 3 orthogonal roots in  $\Phi(E_6)$  are equivalent under  $W(E_6)$ .

2) Any two sets of 3 orthogonal roots in  $\Phi(E_8)$  are equivalent under  $W(E_8)$ .

3) There are two sets of 3 orthogonal roots in  $\Phi(E_7)$  which are not equivalent under  $W(E_7)$ .

*Proof.* We will show that any triple of orthogonal roots in  $E_6$  can be transformed into the triple  $\{\alpha_{max}(E_6), \alpha_{max}(A_5), \alpha_{max}(A_3)\}$ , see Fig. A.44, where  $\alpha_{max}(D)$  means the maximal root in  $\Phi(D)$ . Then any triple of orthogonal roots in  $E_6$  can be transformed into each other. Let  $\{\varphi_1, \varphi_2, \varphi_3\}$  be the triple of orthogonal roots in  $E_6$ . The root  $\varphi_1$  can be transformed into any root in  $W(E_6)$ . We transform  $\varphi_1$  into the maximal root  $\alpha_{max}(E_6)$ . According to Lemma A.4, roots  $\varphi_2$  and  $\varphi_3$  are transformed into two elements in  $\Phi(A_5)$  under  $W(A_5)$ . We transform  $\varphi_2$  into  $\alpha_{max}(A_5)$ , see Fig. A.44. Again, by Lemma A.4,  $\varphi_3$  is transformed under  $W(A_3)$  into the maximal root in  $\Phi(A_3)$ . The root subsets for the case  $E_6$  are:

$$\Phi(E_6) \supset \Phi(A_5) \supset \Phi(A_3).$$

In the case  $E_8$ , we have:

$$\Phi(E_8) \supset \Phi(E_7) \supset \Phi(D_6).$$

In the case  $E_7$ , the subset associated with the third maximal root is split up into 2 non-connected subsets:

$$\Phi(E_7) \supset \Phi(D_6) \supset \Phi(D_4) \oplus \Phi(A_1). \tag{A.2}$$

The decomposition  $\Phi(D_4) \oplus \Phi(A_1)$  in (A.2) is responsible for the presence of two non-equivalent root subsets with 3 orthogonal roots.  $\square$

## REFERENCES

- [BGP73] I. N. Bernstein, I. M. Gelfand, V. A. Ponomarev, *Coxeter functors, and Gabriel's theorem*. (Russian) Uspehi Mat. Nauk 28 (1973), no. 2(170), 19–33. English Translation: Russian Math. Surveys 28 (1973), no. 2, 1732.
- [Bo] N. Bourbaki, *Groupes et algebres de Lie, Chaptires 4, 5, 6*. Paris, Hermann, 1968.
- [B89] P. Bouwknegt, *Lie algebra automorphisms, the weyl group and tables of shift vectors*. J. Math. Phys. 30 (1989), 571–584
- [Ca72] R. W. Carter, *Conjugacy classes in the Weyl group*. Compositio Math. 25 (1972), 1–59
- [CE72] R. W. Carter, G. B. Elkington *A Note on the Parametrization of Conjugacy Classes*. J. Algebra 20 (1972), 350–354
- [Cox91] H. S. M. Coxeter, *The evolution of Coxeter-Dynkin diagrams*. Nieuw Arch. Wisk. (4), 9(3), 233–248, 1991.
- [DF95] F. Delduc, L. Feher, *Regular conjugacy classes in the Weyl group and integrable hierarchies*, J. of Phys. A, vol. 28, n. 20, 1995; arXiv:hep-th/9410203, 1995(v2).
- [DI09] I. V. Dolgachev, V. A. Iskovskikh, *Finite Subgroups of the Plane Cremona Group*, in Algebra, Arithmetic and Geometry: Manin Festschrift (Birkhauser, Boston, 2009), Prog. Math. 269, 270 (in press); math.AG/0610595, 2006 (v1), 2009 (v4).
- [Kac80] V. Kac, *Infinite root systems, representations of graphs and invariant theory*. Invent. Math. 56 (1980), no. 1, 57–92
- [KP85] V. Kac, D. Peterson, *112 constructions of the basic representation of the loop group of  $E_8$* . Symposium on anomalies, geometry, topology (Chicago, Ill., 1985), 276–298, World Sci. Publishing, Singapore, 1985.
- [Men85] V. V. Men'shikh, *Conjugacy in a Weyl group and regularity of representations of graphs*. (Russian) Application of topology in modern analysis (Russian), 144–150, 177, Novoe Global. Anal., Voronezh. Gos. Univ., Voronezh, 1985.
- [Rod04] C. Rodenberg, *Modelle von Flächen dritter Ordnung*, in Mathematische Abhandlungen aus dem Verlage Mathematischer Modelle von Martin Schilling, Halle a. S., 1904.
- [Sev09] A. Sevostyanov, *The structure of the nilpotent cone, the Kazhdan-Lusztig map and algebraic group analogues of the Slodowy slices*, preprint arXiv:0809.0205.
- [St08] R. Stekolshchik, *Notes on Coxeter Transformations and the McKay Correspondence*, Springer Monographs in Mathematics, 2008, XX, 240 p.
- [St10] R. Stekolshchik, *Root systems and diagram calculus. II. Quadratic forms for the Carter diagrams*, arXiv: math.RT/1010.5684v5.
- [St11] R. Stekolshchik, *Root systems and diagram calculus. III. Semi-Coxeter orbits of linkage diagrams and the Carter theorem*, arXiv:math.RT/1105.2875v1.
- [Wi05] A. Wingerter, *Aspects of grand unification in higher dimensions*, Ph.D. thesis, Bonn University, 2005, p. 162.